

Surface Majorana Flat Bands in $j = \frac{3}{2}$ Superconductors with Singlet-Quintet Mixing

Jiabin Yu¹ and Chao-Xing Liu^{1,*}

¹*Department of Physics, the Pennsylvania State University, University Park, PA, 16802*

Recent experiments¹ have revealed the evidence of nodal-line superconductivity in half-Heusler superconductors, e.g. YPtBi. Theories have suggested the topological nature of such nodal-line superconductivity and proposed the existence of surface Majorana flat bands on the (111) surface of half-Heusler superconductors. Due to the divergent density of states of the surface Majorana flat bands, the surface order parameter and the surface impurity play essential roles in determining the surface properties. In this work, we studied the effect of the surface order parameter and the surface impurity on the surface Majorana flat bands of half-Heusler superconductors based on the Luttinger model. To be specific, we consider the topological nodal-line superconducting phase induced by the singlet-quintet pairing mixing, classify all the possible translationally invariant order parameters for the surface states according to irreducible representations of C_{3v} point group, and demonstrate that any energetically favorable order parameter needs to break time-reversal symmetry. We further discuss the energy splitting in the energy spectrum of surface Majorana flat bands induced by different order parameters and non-magnetic or magnetic impurities. We proposed that the splitting in the energy spectrum can serve as the fingerprint of the pairing symmetry and mean-field order parameters. Our theoretical prediction can be examined in the future scanning tunneling microscopy experiments.

I. Introduction

Recent years have witnessed increasing research interests in half-Heusler compounds ($RPdBi$ or $RPtBi$ with R a rare-earth element)² due to their non-trivial band topology^{3–16}, magnetism^{17–25} and unconventional superconductivity^{1,17,20–22,26–33}. Half-Heusler superconductors (SCs) are of particular interest because of the low carrier density ($10^{18} \sim 10^{19} \text{cm}^{-3}$), the power-law temperature dependence of London penetration depth, and the large upper critical field. Furthermore, it was theoretically proposed that electrons near Fermi level in half-Heusler SCs possess total angular momentum $j = \frac{3}{2}$ as a result of the addition of the $\frac{1}{2}$ spin and the angular momentum of p atomic orbitals ($l = 1$).^{1,34} Therefore, half-Heusler SCs provide a great platform to study the superconductivity of $j = \frac{3}{2}$ fermions. Such $j = \frac{3}{2}$ fermions were also studied in anti-perovskite materials³⁵ and the cold atom system^{36,37}. Due to the $j = \frac{3}{2}$ nature, the spin of Cooper pairs can take four values: $S = 0$ (singlet), 1 (triplet), 2 (quintet) and 3 (septet), among which quintet and septet Cooper pairs cannot appear for spin- $\frac{1}{2}$ electrons.

In order to understand the unconventional superconductivity, various pairing states were proposed, including mixed singlet-septet pairing^{1,34,38,39}, mixed singlet-quintet pairing^{40–42}, s-wave quintet pairing^{34,39,43,44}, d-wave quintet pairing^{45,46}, odd-parity (triplet and septet) pairings^{45–48}, *et al*^{46,49}. In particular, Ref. [1, 34, 38–42] proposed that the power-law temperature dependence of London penetration depth can be explained by topological nodal-line superconductivity (TNLS) generated by the pairing mixing between different spin channels. In particular, it has been shown that two types of pairing mixing states, the singlet-quintet mixing and singlet-septet mixing, can both give rise to nodal lines in certain

parameter regimes.

In this work, we focus on the singlet-quintet mixing, which was proposed in Ref. [40]. As a consequence of TNLS, the Majorana flat bands (MFBs) are expected to exist on the surface perpendicular to certain directions. Such surface MFBs (SMFBs) are expected to show divergent quasi-particle density of states (DOS) at the Fermi energy and thus can be directly probed through experimental techniques, such as scanning tunneling microscopy (STM).⁵⁰ Due to the divergent DOS, certain types of interaction^{51–54} and surface impurities^{55–57} are expected to have a strong influence on SMFBs. This motivates us to study the effect of the interaction-induced surface order parameter and the surface impurity on the SMFBs of the superconducting Luttinger model with the singlet-quintet mixing. Specifically, we classify all the mean-field translationally invariant order parameters of the SMFBs according to the irreducible representations (IRs) of C_{3v} group, identify their possible physical origins, and show their energy spectrum by calculating the corresponding DOS. We find that the order parameter needs to break the time-reversal (TR) symmetry in order to either gap out the SMFBs or convert the SMFBs to nodal-lines or nodal points. We also study the quasi-particle local DOS (LDOS) of SMFBs with a surface charge impurity or a surface magnetic impurity (whose magnetic moment is perpendicular to the surface), and show that the peak splitting induced by different types of impurities can help to distinguish the pairing symmetries and surface order parameters.

The rest of the paper is organized as the following. In Sec. II and III, we briefly review the superconducting Luttinger model with singlet-quintet mixing and illustrate the symmetry properties of SMFBs. In Sec. IV, we classify all the mean-field translationally invariant order parameters according to the IRs of C_{3v} and identify their physical origin. We also calculate the energy spec-

trum and DOS of SMFBs with different order parameters. In Sec. V, the impurity effect on the LDOS of MFBs with/without the surface order parameter is discussed. Finally, our work is concluded in Sec. VI

II. Model Hamiltonian

The model that we used to generate MFBs in this work is the same as that studied in Ref. [40], which describes the superconductivity in the Luttinger model with mixed s-wave singlet and isotropic d-wave quintet channels. The Bogoliubov-de-Gennes (BdG) Hamiltonian in the continuous limit reads

$$H = \frac{1}{2} \sum_{\mathbf{k}} \Psi_{\mathbf{k}}^\dagger h_{BdG}(\mathbf{k}) \Psi_{\mathbf{k}} + const., \quad (1)$$

where $\Psi_{\mathbf{k}}^\dagger = (c_{\mathbf{k}}^\dagger, c_{-\mathbf{k}}^T)$ is the Nambu spinor and $c_{\mathbf{k}}^\dagger = (c_{\mathbf{k},\frac{3}{2}}^\dagger, c_{\mathbf{k},\frac{1}{2}}^\dagger, c_{\mathbf{k},-\frac{1}{2}}^\dagger, c_{\mathbf{k},-\frac{3}{2}}^\dagger)$ are creation operators of $j = \frac{3}{2}$ fermionic excitations. The term

$$h_{BdG}(\mathbf{k}) = \begin{pmatrix} h(\mathbf{k}) & \Delta(\mathbf{k}) \\ \Delta^\dagger(\mathbf{k}) & -h^T(-\mathbf{k}) \end{pmatrix} \quad (2)$$

consists of the normal part $h(\mathbf{k})$ that is the Luttinger model^{4,40,58,59}

$$h(\mathbf{k}) = \left(\frac{k^2}{2m} - \mu\right)\Gamma^0 + c_1 \sum_{i=1}^3 g_{\mathbf{k},i} \Gamma^i + c_2 \sum_{i=4}^5 g_{\mathbf{k},i} \Gamma^i \quad (3)$$

and the pairing part $\Delta(\mathbf{k})$ that contains s-wave singlet and isotropic d-wave quintet channels

$$\Delta(\mathbf{k}) = \Delta_0 \frac{\Gamma^0}{2} \gamma + \Delta_1 \sum_{i=1}^5 \frac{a^2 g_{\mathbf{k},i} \Gamma^i}{2} \gamma, \quad (4)$$

where μ is the chemical potential, c_1, c_2 indicate the strength of the centrosymmetric spin orbital coupling (SOC) which is the coupling between the orbital and the 3/2-“spin”, d-wave cubic harmonics $g_{\mathbf{k},i}$ and five Γ matrices are shown in Appendix A, $\Delta_{0,1}$ are order parameters of singlet and quintet channels, respectively, a is the lattice constant of the material, and $\gamma = -\Gamma^1 \Gamma^3$ is the TR matrix. The coexistence of the two order parameters is allowed by their same symmetry properties^{40,60–66}.

Before demonstrating the SMFB generated by Eq. (1), we first discuss the symmetry properties of the Hamiltonian H . As discussed in Ref. [40], H has TR symmetry, and its point group is $O(3)$ or O_h for $c_1 = c_2$ or $c_1 \neq c_2$, respectively. Due to the coexistence of TR and inversion symmetries, the Luttinger model $h(\mathbf{k})$ has two doubly degenerate bands $\xi_{\pm}(\mathbf{k}) = k^2/(2m_{\pm}) - \mu$, where $m_{\pm} = m\tilde{m}_{\pm}$ are effective masses of two bands, $\tilde{m}_{\pm} = 1/(1 \pm 2mQ_c)$, $Q_c = \sqrt{c_1^2 Q_1^2 + c_2^2 Q_2^2}$, $Q_1 = \sqrt{\hat{g}_1^2 + \hat{g}_2^2 + \hat{g}_3^2}$, $Q_2 = \sqrt{\hat{g}_4^2 + \hat{g}_5^2}$, and $\hat{g}_i = g_i/k^2$. In addition, particle-hole (PH) symmetry can be defined as

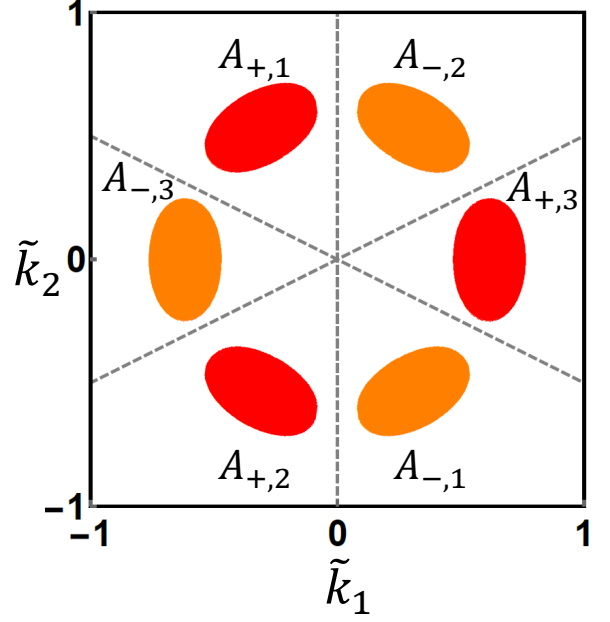


FIG. 1. This is the distribution of SMFBs for $|2m|c_1 = 0.8$, $|2m|c_2 = 0.5$, $\tilde{\Delta}_0/|\mu| = 1$ and $\tilde{\Delta}_1/|\mu| = 1.6$, where $\tilde{\Delta}_0 = \text{sgn}(c_1)\Delta_0$, $\tilde{\Delta}_1 = 2m\mu a^2 \Delta_1$ and $\tilde{k}_{1,2} = k_{1,2}/\sqrt{2m\mu}$. The surface zero modes in red (orange) regions have 1 (−1) chiral eigenvalue, and $A^{lc,lx}$ ’s are labeled according to the convention. The dashed lines are given by $k_{||,1} = 0$ and $k_{||,2} = \pm k_{||,1}/2$, where the surface zero modes cannot exist.

$-\mathcal{C}h_{BdG}^*(-\mathbf{k})\mathcal{C}^\dagger = h_{BdG}(\mathbf{k})$ and $\Psi_{\mathbf{k}}^\dagger \mathcal{C} = \Psi_{-\mathbf{k}}^T$ for the BdG Hamiltonian, where $\mathcal{C} = \tau_x$ with τ_x the Pauli matrix for the PH index. Combining the PH and TR symmetries, we have the chiral symmetry $-\chi h_{BdG}(\mathbf{k})\chi^\dagger = h_{BdG}(\mathbf{k})$, where $\chi = i\mathcal{T}\mathcal{C}^*$ and $\mathcal{T} = \text{diag}(\gamma, \gamma^*)$ is the TR matrix on the Nambu bases. The representations of other symmetry operators are shown in Appendix B.

III. Surface Majorana Flat Bands

In this work, we choose $\mu < 0$, $m < 0$ and $c_1 c_2 > 0$, and focus on the case where $c_1 \neq c_2$, $m_{\pm} < 0$, and SMFBs exist on the (111) surface.⁴⁰ To solve for SMFBs, we consider a semi-infinite configuration ($x_{\perp} < 0$) of Eq. (1) along the (111) direction with an open boundary condition at the $x_{\perp} = 0$ surface, where x_{\perp} labels the position along (111). In this case, the point group is reduced from O_h to C_{3v} , which is generated by three-fold rotation \hat{C}_3 along the (111) direction and the mirror operation $\hat{\Pi}$ perpendicular to the $(\bar{1}10)$ direction. Although the translational invariance along (111) is broken, the momentum $\mathbf{k}_{||}$ that lies inside the (111) plane is still a good quantum number, and we define $k_{||,1}$ and $k_{||,2}$ along the (112) and $(\bar{1}10)$ directions, respectively.

Following Ref. [40], we find that SMFBs can exist in certain regions of the surface Brillouin zone, denoted

as A in Fig. 1, and originate from the non-trivial one-dimensional AIII bulk topological invariant ($N_w = \pm 2$). At each $\mathbf{k}_\parallel \in A$, the semi-infinite model has two orthonormal solutions of zero energy that are localized near the $x_\perp = 0$ surface and have the same chiral eigenvalues, coinciding with the bulk topological invariant $N_w = \pm 2$.

We label the creation operators for the two zero-energy solutions at $\mathbf{k}_\parallel \in A$ as $b_{i,\mathbf{k}_\parallel}^\dagger$ with $i = 1, 2$, and they satisfy the anti-commutation relation

$$\{b_{i,\mathbf{k}_\parallel}^\dagger, b_{j,\mathbf{k}'_\parallel}\} = \delta_{ij} \delta_{\mathbf{k}_\parallel, \mathbf{k}'_\parallel} . \quad (5)$$

The subscript $i = 1, 2$ of $b_{i,\mathbf{k}_\parallel}^\dagger$ can be regarded as the pseudospin index, since $b_{i,\mathbf{k}_\parallel}^\dagger$ can furnish the same representation of TR, \hat{C}_3 and $\hat{\Pi}$ operators as a two dimensional $j = 1/2$ fermion by choosing the convention

$$\begin{cases} \hat{\mathcal{T}} b_{\mathbf{k}_\parallel}^\dagger \hat{\mathcal{T}}^{-1} = b_{-\mathbf{k}_\parallel}^\dagger \mathcal{T}_b \\ \hat{C}_3 b_{\mathbf{k}_\parallel}^\dagger \hat{C}_3^{-1} = b_{C_3 \mathbf{k}_\parallel}^\dagger C_{3,b} \\ \hat{\Pi} b_{\mathbf{k}_\parallel}^\dagger \hat{\Pi}^{-1} = b_{\Pi \mathbf{k}_\parallel}^\dagger \Pi_b \end{cases} , \quad (6)$$

where $\mathcal{T}_b = i\sigma_2$, $C_{3,b} = e^{-i\sigma_3 \frac{\pi}{3}}$, $\Pi_b = -e^{-i\sigma_2 \frac{\pi}{2}}$, and $\sigma_{1,2,3}$ are Pauli matrices for the pseudospin of SMFBs. Since the chiral matrix χ commutes with any operation in C_{3v} and anti-commutes with TR operation, the chiral eigenvalue of $b_{i,\mathbf{k}_\parallel}^\dagger$ is the same as $b_{i,R\mathbf{k}_\parallel}^\dagger$, but opposite to $b_{i,-\mathbf{k}_\parallel}^\dagger$, where $R \in C_{3v}$. As a result, the surface zero-energy modes cannot exist on three lines parametrized by $k_{\parallel,1} = 0$ and $k_{\parallel,2} = \pm k_{\parallel,1}/2$, dividing the region A into six patches as shown in Fig. 1. Since the chiral eigenvalues of the zero-energy modes in one patch are the same, we can label each patch as A_{l_χ, l_c} with $l_\chi = \pm$ for the chiral eigenvalues ± 1 and $l_c = 1, 2, 3$ marking three patches related by \hat{C}_3 rotation. Furthermore, we choose $A_{l_\chi, 3}$ to be symmetric under $k_{\parallel,2} \rightarrow -k_{\parallel,2}$, i.e. the mirror operation perpendicular to $(\bar{1}10)$. Due to the PH symmetry, the surface zero modes at $\pm \mathbf{k}_\parallel$ are related by

$$b_{\mathbf{k}_\parallel}^\dagger (-\delta_{\mathbf{k}_\parallel}^x \sigma_2) = b_{-\mathbf{k}_\parallel}^T , \quad (7)$$

where $\delta_{\mathbf{k}_\parallel}^x$ is the chiral eigenvalue of the zero modes at \mathbf{k}_\parallel , i.e. $\delta_{\mathbf{k}_\parallel}^x = \pm 1$ for $\mathbf{k}_\parallel \in A_\pm$ with $A_{l_\chi} = \cup_{l_c} A_{l_\chi, l_c}$. TR and C_{3v} symmetries imply $\delta_{-\mathbf{k}_\parallel}^x = -\delta_{\mathbf{k}_\parallel}^x$ and $\delta_{R\mathbf{k}_\parallel}^x = \delta_{\mathbf{k}_\parallel}^x$ with $R \in C_{3v}$. (See Appendix C for details.)

IV. Mean-field Order Parameters of Surface Majorana Flat Bands

Due to the divergent DOS, the interaction may result in the nonvanishing order parameters at the surface and give rise to a gap of SMFBs. In this section, we study the possible mean-field order parameters on the (111) surface that preserve the in-plane translation symmetry. We find that the order parameters must break the TR

symmetry in order to gap out the SMFB; all the TR-breaking surface order parameters are classified based on the IRs of C_{3v} and their physical origins are identified. Then, to the leading order approximation where the surface order parameters are independent of \mathbf{k}_\parallel in each of the surface mode regions, we find the SMFBs can be generally gapped out by these order parameters, and the gapless modes are only possible for certain IRs with certain finely tuned values of parameters. We further study the LDOS structure of SMFBs in the presence of various order parameters and find the splitting patterns of the LDOS peak can be used to distinguish different order parameters as summarized in Fig. 2 and 4.

A. Symmetry Classification and Physical Origin

The general form of translationally invariant fermion-bilinear terms for SMFBs can be constructed as

$$H_{mf} = \frac{1}{2} \sum_{\mathbf{k}_\parallel \in A} b_{\mathbf{k}_\parallel}^\dagger m(\mathbf{k}_\parallel) b_{\mathbf{k}_\parallel} + \text{const.} , \quad (8)$$

where $m(\mathbf{k}_\parallel)$ is a 2×2 Hermitian matrix. The PH symmetry makes $m(\mathbf{k}_\parallel)$ satisfy $m(\mathbf{k}_\parallel) = -\sigma_2 m^T(-\mathbf{k}_\parallel) \sigma_2$ up to a shift of ground state energy based on Eq. (7), while TR symmetry requires $\mathcal{T}_b m^*(-\mathbf{k}_\parallel) \mathcal{T}_b^\dagger = m(\mathbf{k}_\parallel)$ according to Eq. (6). As a result, the combination of PH and TR symmetries, which is equivalent to the chiral symmetry, leads to $m(\mathbf{k}_\parallel) = 0$, indicating that the existence of a non-vanishing fermion bilinear term $m(\mathbf{k}_\parallel)$ for the SMFBs requires the breaking of TR symmetry, i.e.

$$\mathcal{T}_b m^*(-\mathbf{k}_\parallel) \mathcal{T}_b^\dagger = -m(\mathbf{k}_\parallel) . \quad (9)$$

As the C_{3v} point group symmetry can also be spontaneously broken by these fermion-bilinear terms, we can further classify these TR-breaking order parameters according to the IR of C_{3v} , of which the character table (Tab. II) is shown in Appendix A. Since C_{3v} has three IRs A_1 , A_2 and E , Eq. (8) can be expressed as the linear combination of the three corresponding parts

$$m(\mathbf{k}_\parallel) = m_{A_1}(\mathbf{k}_\parallel) + m_{A_2}(\mathbf{k}_\parallel) + m_E(\mathbf{k}_\parallel) . \quad (10)$$

Here the A_1 term $m_{A_1}(\mathbf{k}_\parallel)$ preserves C_{3v} symmetry, and the A_2 term $m_{A_2}(\mathbf{k}_\parallel)$ preserves \hat{C}_3 symmetry but has odd mirror parity. The E term has the expression $m_E(\mathbf{k}_\parallel) = a_1 m_{E,1}(\mathbf{k}_\parallel) + a_2 m_{E,2}(\mathbf{k}_\parallel)$ with $(m_{E,1}(\mathbf{k}_\parallel), m_{E,2}(\mathbf{k}_\parallel))$ a two-component vector that can furnish a E IR; it breaks the entire C_{3v} symmetry except for some special values of (a_1, a_2) , e.g. one of the three mirrors is preserved but the \hat{C}_3 is broken for $(a_1, a_2) \propto (1, 0), (1, \sqrt{3})$ or $(1, -\sqrt{3})$.

Next we illustrate the physical origin of each term in Eq. (10) by considering the following on-site mean-field

Hamiltonian that are independent of \mathbf{k}_\parallel

$$\begin{aligned} \tilde{H}_{mf} = & \sum_{\mathbf{k}_\parallel} \int_{-\infty}^0 dx_\perp [c_{\mathbf{k}_\parallel, x_\perp}^\dagger \tilde{M}(x_\perp) c_{\mathbf{k}_\parallel, x_\perp} + \\ & \frac{1}{2} c_{\mathbf{k}_\parallel, x_\perp}^\dagger \tilde{D}(x_\perp) (c_{-\mathbf{k}_\parallel, x_\perp}^\dagger)^T + \frac{1}{2} c_{-\mathbf{k}_\parallel, x_\perp}^T \tilde{D}^\dagger(x_\perp) c_{\mathbf{k}_\parallel, x_\perp}] , \end{aligned} \quad (11)$$

where $\tilde{M}^\dagger(x_\perp) = \tilde{M}(x_\perp)$ and $-\tilde{D}^T(x_\perp) = \tilde{D}(x_\perp)$. Eq. (8) can be obtained by projecting the above Hamiltonian onto the surface, and such projection does not change the symmetry properties. Since $m(\mathbf{k}_\parallel)$ must be TR odd in order to be non-vanishing, it requires $\tilde{M}(x_\perp)$ and $\tilde{D}(x_\perp)$ to be TR odd. Then, the TR-breaking \tilde{M} and \tilde{D} can be classified into different IRs of C_{3v} :

$$\tilde{M}(x_\perp) = \tilde{M}_{A_1}(x_\perp) + \tilde{M}_{A_2}(x_\perp) + \tilde{M}_E(x_\perp) , \quad (12)$$

and

$$\tilde{D}(x_\perp) = \tilde{D}_{A_1}(x_\perp) + \tilde{D}_{A_2}(x_\perp) + \tilde{D}_E(x_\perp) , \quad (13)$$

where $\tilde{M}_\beta(x_\perp)$ and $\tilde{D}_\beta(x_\perp)$ can only give rise to $m_\beta(\mathbf{k}_\parallel)$ in Eq. (10) with $\beta = A_1, A_2, E$. (See Appendix.D for details.) Concretely, we have

$$\left\{ \begin{array}{l} \tilde{M}_{A_1}(x_\perp) = \zeta_2(x_\perp) n_2 \\ \tilde{M}_{A_2}(x_\perp) = \sum_{j=3}^5 \zeta_j(x_\perp) n_j \\ \tilde{M}_E(x_\perp) = \sum_{j=8}^{10} \zeta_j(x_\perp) \cdot \mathbf{n}_j \\ \tilde{D}_{A_1}(x_\perp) = \sum_{j=0}^1 i \zeta_j(x_\perp) n_j \gamma \\ \tilde{D}_{A_2}(x_\perp) = 0 \\ \tilde{D}_E(x_\perp) = \sum_{j=6}^7 i \zeta_j(x_\perp) \cdot \mathbf{n}_j \gamma \end{array} \right. , \quad (14)$$

where n_i 's are listed in Tab.III of Appendix.A, and $\zeta_j(x_\perp)$'s are real. Physically, $n_0\gamma$ corresponds to the singlet pairing, $n_1\gamma$, $\mathbf{n}_6\gamma$ and $\mathbf{n}_7\gamma$ generate quintet pairings, and $n_4, n_{8,1}, n_{8,2}$ give FM in (111), (110) and (112) directions, respectively. Since $n_2, n_3, n_5, \mathbf{n}_9$ and \mathbf{n}_{10} can be represented by the linear combinations of $c_{\mathbf{k}_\parallel, x_\perp}^\dagger S^{3m} c_{\mathbf{k}_\parallel, x_\perp}$ with the septet spin tensor S^{3m} ($m = -3, -2, \dots, 3$), we dub these terms the spin-septet order parameters. As a summary, $m_{A_1}(\mathbf{k}_\parallel)$ can be generated by the singlet pairing, the quintet pairing, and the spin-septet order parameter; $m_{A_2}(\mathbf{k}_\parallel)$ can be generated by (111)-directional ferromagnetism (FM) and the spin-septet order parameter; $m_E(\mathbf{k}_\parallel)$ can be generated by the quintet pairing, the FM perpendicular to the (111) direction, and the spin-septet order parameter.

B. Surface Local Density of States

In the following, we focus on the order parameters that are independent of \mathbf{k}_\parallel in every one of six surface mode regions A_{l_χ, l_c} 's. In this case, Eq. (10) can be expanded

C_{3v}	Bases	TR	PH	χ
A_1	$\sum_{l_\chi, l_c} \delta_{\mathbf{k}_\parallel}^{l_\chi l_c} = 1$ for $\mathbf{k}_\parallel \in A$	+	+	+
A_1	$\delta_{\mathbf{k}_\parallel}^{\chi} = \sum_{l_\chi, l_c} l_\chi \delta_{\mathbf{k}_\parallel}^{l_\chi l_c}$	-	-	+
E	$(\delta_{\mathbf{k}_\parallel}^{E_{1,+}}, \delta_{\mathbf{k}_\parallel}^{E_{2,+}})$	+	+	+
E	$(\delta_{\mathbf{k}_\parallel}^{E_{1,-}}, \delta_{\mathbf{k}_\parallel}^{E_{2,-}})$	-	-	+
A_1	σ_0	+	+	+
A_2	σ_3	-	-	+
E	$(-\sigma_2, \sigma_1)$	-	-	+
A_1	ρ_0	+	+	+
A_1	ρ_1	+	-	-
A_1	ρ_2	+	-	-
A_1	ρ_3	-	-	+
A_1	$\Lambda_1 = \lambda_0$	+	+	+
A_1	$\Lambda_2 = \frac{1}{\sqrt{2}}(\lambda_1 + \lambda_4 + \lambda_6)$	+	+	+
A_2	$\Lambda_3 = \frac{1}{\sqrt{2}}(\lambda_2 - \lambda_5 + \lambda_7)$	-	-	+
E	$\Lambda_4 = \frac{\sqrt{3}}{2}(\lambda_8, -\lambda_3)$	+	+	+
E	$\Lambda_5 = \sqrt{\frac{3}{8}}(\lambda_5 + \lambda_7, \frac{-2\lambda_2 - \lambda_5 + \lambda_7}{\sqrt{3}})$	-	-	+
E	$\Lambda_6 = \sqrt{\frac{3}{8}}(\frac{-2\lambda_1 + \lambda_4 + \lambda_6}{\sqrt{3}}, \lambda_4 - \lambda_6)$	+	+	+

TABLE I. The irreducible representations of C_{3v} generated by $\delta_{\mathbf{k}_\parallel}^{l_\chi l_c}$, σ_l , ρ_l or λ_l with their parities under TR, PH and chiral operation. The transformation of $\delta_{\mathbf{k}_\parallel}^{l_\chi l_c}$ is defined as $\delta_{\mathbf{k}_\parallel}^{l_\chi l_c} \rightarrow \delta_{R^{-1}\mathbf{k}_\parallel}^{l_\chi l_c}$, the transformation of σ_l is $\sigma_l \rightarrow R_b \sigma_l R_b^\dagger$, the transformation of ρ_l is $\rho_l \rightarrow R_\chi \rho_l R_\chi^\dagger$ and the transformation of λ_l is $\lambda_l \rightarrow R_c \lambda_l R_c^\dagger$, where $R = -1, -1, 1, C_3, \Pi$, $R_b = i\sigma_2 K, \sigma_2 K, \mathbb{1}, C_{3,b}, \Pi_b$, $R_\chi = \mathcal{T}_\chi K, C_\chi K, \chi_\chi, C_{3,\chi}, \Pi_\chi$ and $R_c = \mathcal{T}_c K, C_c K, \chi_c, C_{3,c}, \Pi_c$ for TR, PH, χ , C_3 and Π , respectively, and K is the complex conjugate operation. The parity $\alpha = \pm$ is defined as $X \rightarrow \alpha X$ under the operation of TR, PH or χ and thus being TR, PH and χ symmetric correspond to $\alpha = +, -, -$, respectively. $l_\chi = \pm$, $l_c = 1, 2, 3$ and $\delta_{\mathbf{k}_\parallel}^{l_\chi l_c}$ is equal to 1 if $\mathbf{k}_\parallel \in A_{l_\chi, l_c}$ and 0 otherwise. $(\delta_{\mathbf{k}_\parallel}^{E_{1,+}}, \delta_{\mathbf{k}_\parallel}^{E_{2,+}}) = (\sum_{l_\chi} \frac{1}{2}(\delta_{\mathbf{k}_\parallel}^{l_\chi, 1} + \delta_{\mathbf{k}_\parallel}^{l_\chi, 2} - 2\delta_{\mathbf{k}_\parallel}^{l_\chi, 3}), \sum_{l_\chi} \frac{\sqrt{3}}{2}(-\delta_{\mathbf{k}_\parallel}^{l_\chi, 1} + \delta_{\mathbf{k}_\parallel}^{l_\chi, 2}))$ and $(\delta_{\mathbf{k}_\parallel}^{E_{1,-}}, \delta_{\mathbf{k}_\parallel}^{E_{2,-}}) = (\sum_{l_\chi} \frac{l_\chi}{2}(\delta_{\mathbf{k}_\parallel}^{l_\chi, 1} + \delta_{\mathbf{k}_\parallel}^{l_\chi, 2} - 2\delta_{\mathbf{k}_\parallel}^{l_\chi, 3}), \sum_{l_\chi} \frac{l_\chi \sqrt{3}}{2}(-\delta_{\mathbf{k}_\parallel}^{l_\chi, 1} + \delta_{\mathbf{k}_\parallel}^{l_\chi, 2}))$.

as

$$m(\mathbf{k}_\parallel) = \sum_{l=0}^4 \sum_{l_\chi = \pm} \sum_{l_c=1}^3 f_l^{l_\chi l_c} \sigma_l \delta_{\mathbf{k}_\parallel}^{l_\chi l_c} , \quad (15)$$

where $f_l^{l_\chi l_c}$ is real, $\delta_{\mathbf{k}_\parallel}^{l_\chi l_c} = 1$ if $\mathbf{k}_\parallel \in A_{l_\chi, l_c}$ and $\delta_{\mathbf{k}_\parallel}^{l_\chi l_c} = 0$ otherwise, and σ_l labels the Pauli matrix for pseudospin. Then, for any symmetry transformation of $m(\mathbf{k})$, we can convert the transformation of pseudospin index and \mathbf{k}_\parallel dependence of $m(\mathbf{k})$ to the transformation of σ_l and $\delta_{\mathbf{k}_\parallel}^{l_\chi l_c}$,

respectively. Based on the symmetry transformation, we can classify $\delta_{\mathbf{k}_\parallel}^{l_\chi l_c}$ and σ_l according to the IRs of C_{3v} and the parities under TR, PH and χ , as shown in the top and second top parts of Tab. I, respectively. The symmetry classification of TR-odd terms in $m(\mathbf{k}_\parallel)$ can be obtained by the tensor product of σ_l and $\delta_{\mathbf{k}_\parallel}^{l_\chi l_c}$, as shown in Tab. IV of Appendix. A with various terms labeled by N_i 's. As a result, we have the following general expressions of the order parameters in different IRs of C_{3v} :

$$m_{A_1}(\mathbf{k}_\parallel) = \sum_{j=1}^2 m_j N_j(\mathbf{k}_\parallel), \quad (16)$$

$$m_{A_2}(\mathbf{k}_\parallel) = \sum_{j=3}^4 m_j N_j(\mathbf{k}_\parallel), \quad (17)$$

and

$$m_E(\mathbf{k}_\parallel) = \sum_{j=5}^8 \mathbf{m}_j \cdot \mathbf{N}_j(\mathbf{k}_\parallel). \quad (18)$$

Here all m_j 's are real.

With Eq. (16)-(18), we next discuss the energy spectrum and LDOS of SMFBs after including these order parameters. Due to the PH symmetry, only half of the energy spectrum (non-negative energy part) gives the quasi-particle LDOS of SMFBs. However, it is more convenient to study the full spectrum, since the LDOS, which is probed by the tunneling conductance of STM, must symmetrically distribute with respect to the zero energy in experiments⁶⁷. Since the order parameters in each patch are \mathbf{k}_\parallel -independent, we choose the mode at the geometric center $\mathbf{K}_\parallel^{l_\chi, l_c}$ of each patch A_{l_χ, l_c} as the representative mode. In the following, we only consider the representative modes and use the term “degeneracy” to refer to the *extra* degeneracy determined by the symmetry, excluding the large degeneracy given by the flatness of the dispersion in each patch. For convenience, we define the creation operator $b_{i, l_\chi, l_c}^\dagger = b_{i, \mathbf{K}_\parallel^{l_\chi, l_c}}^\dagger$ to label the representative mode in the patch A_{l_χ, l_c} with the pseudo-spin index i . Since only the uniform order parameters are considered, l_χ and l_c are good quantum numbers, while different pseudo-spin components (the σ_l part) are typically coupled by the order parameter $m(\mathbf{k}_\parallel)$. Thus, we introduce the band index $s = \pm$ and label the eigen-mode as $\tilde{b}_{s, l_\chi, l_c}^\dagger = \sum_i X_i^{s, l_\chi, l_c} b_{i, l_\chi, l_c}^\dagger$ with

$$\sum_{l_\chi, l_c} m(\mathbf{K}_\parallel^{l_\chi, l_c}) X^{s, l_\chi, l_c} = \sum_{l_\chi, l_c} E^{s, l_\chi, l_c} X^{s, l_\chi, l_c} \quad (19)$$

the eigen-equation.

Without any order parameters, all these 12 modes, including 6 patches and 2 pseudospin components, are degenerate and thus the SMFBs has a zero-bias peak for LDOS, as shown in Fig. 2a. For the A_1 order $m_{A_1}(\mathbf{k}_\parallel)$,

the eigen-energies are given by $m_1 \delta_{\mathbf{k}_\parallel}^\chi \pm |m_2|$, and once $|m_1| \neq |m_2|$, all the zero energy peaks will be split for SMFBs. As a result, the LDOS of the A_1 order parameter typically has 4 peaks shown in Fig. 2b. This peak structure of LDOS can be understood from symmetry consideration. Due to the breaking of TR symmetry, as well as the chiral symmetry, we only need to consider the the point group symmetry C_{3v} . As mentioned before, any operation in C_{3v} does not change the l_χ index, and since A_1 order parameter is C_{3v} invariant, the band index s cannot be changed either. The C_3 rotation only transforms the $l_c = 1, 2, 3$ index counter-clockwise, resulting in the three-fold degeneracy among the eigen-modes $\tilde{b}_{s, l_\chi, l_c}^\dagger$ with the same s and l_χ . On the other hand, Π interchanges $l_c = 1, 2$ and makes sure $\tilde{b}_{s, l_\chi, 1}^\dagger$ has the same energy as $\tilde{b}_{s, l_\chi, 2}^\dagger$, meaning that Π does not give extra constraints compared with C_3 . Thus, there are $12/3 = 4$ peaks in the LDOS of the A_1 order parameter with each peak of 3-fold degeneracy. For the A_2 order parameter $m_{A_2}(\mathbf{k}_\parallel)$, the eigen-energies are given by $\pm \sqrt{m_3^2 + m_4^2}$, leading to 2 peaks in the LDOS (Fig. 2c), resulted from the six-fold degeneracy of each eigen-energy due to the symmetry. Among the six-fold degeneracy, three-fold degeneracy is due to translational invariance and C_3 symmetry as the A_1 order parameter, meaning that $\tilde{b}_{s, l_\chi, 1}^\dagger$, $\tilde{b}_{s, l_\chi, 2}^\dagger$ and $\tilde{b}_{s, l_\chi, 3}^\dagger$ have the same energy. The remaining double degeneracy originates from the combination of the odd mirror parity of the A_2 order parameter and the PH symmetry, i.e. $\Pi_b \sigma_2 m_{A_2}^* (-\Pi^{-1} \mathbf{k}_\parallel) (\Pi_b \sigma_2)^\dagger = m_{A_2}(\mathbf{k}_\parallel)$. This combined symmetry does not change the band index s , but transforms l_χ as $+\leftrightarrow -$ and l_c as $1 \leftrightarrow 2$. As a result, $\tilde{b}_{s, \pm, l_c}^\dagger$ with fixed s and l_c also have the same energy, giving the extra double degeneracy. For the E order parameter $m_E(\mathbf{k}_\parallel)$, the eigen-energies are $\sum_{l_\chi, l_c} (l_\chi \bar{m}_{l_c} \pm \bar{m}'_{l_c}) \delta_{\mathbf{k}_\parallel}^{l_\chi, l_c}$, where

$$\begin{aligned} \bar{m}_1 &= \frac{m_{5,1}}{2} - \frac{\sqrt{3}}{2} m_{5,2} \\ \bar{m}_2 &= \frac{m_{5,1}}{2} + \frac{\sqrt{3}}{2} m_{5,2}, \quad \bar{m}_3 = -m_{5,1} \\ \bar{m}'_1 &= [(\frac{\sqrt{3}}{2} m_{6,1} + \frac{m_{6,2}}{2})^2 + (-m_{7,1} + \frac{m_{8,1}}{2} + \frac{\sqrt{3}}{2} m_{8,2})^2 \\ &\quad + (m_{7,2} - \frac{\sqrt{3}}{2} m_{8,1} + \frac{m_{8,2}}{2})^2]^{1/2} \\ \bar{m}'_2 &= [(-\frac{\sqrt{3}}{2} m_{6,1} + \frac{m_{6,2}}{2})^2 + (-m_{7,1} + \frac{m_{8,1}}{2} - \frac{\sqrt{3}}{2} m_{8,2})^2 \\ &\quad + (m_{7,2} + \frac{\sqrt{3}}{2} m_{8,1} + \frac{m_{8,2}}{2})^2]^{1/2} \\ \bar{m}'_3 &= [m_{6,2}^2 + (m_{7,1} + m_{8,1})^2 + (m_{7,2} - m_{8,2})^2]^{1/2}. \end{aligned} \quad (20)$$

Therefore, all the modes are typically split for the E order and the corresponding LDOS generally has 12 peaks shown in Fig. 2d.

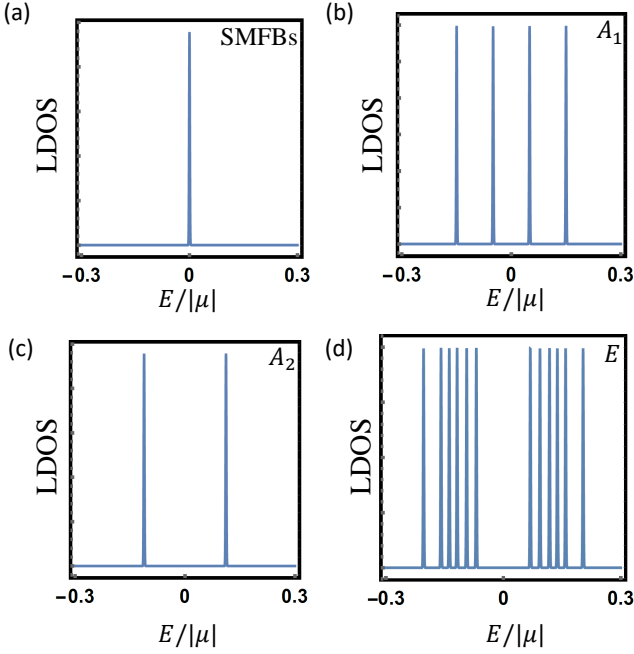


FIG. 2. (a), (b), (c) and (d) show the LDOS on the (111) surface as a function of the energy ($E/|\mu|$) without any order parameters, with the A_1 order parameter, with the A_2 order parameter and with the E order parameter, respectively. Due to PH symmetry, only non-negative-energy half of the LDOS is physical. The broadening of each peak is plotted via Gaussian distribution with standard deviation being 10^{-3} . The parameters choices for each order if exist are $m_1/|\mu| = 0.05$ and $m_2/|\mu| = 0.1$ for the A_1 order parameter (16), $m_3/|\mu| = 0.05$ and $m_4/|\mu| = -0.1$ for the A_2 order parameter (17), and $m_5/|\mu| = (0.01, 0.02)$, $m_6/|\mu| = (0.03, 0.04)$, $m_7/|\mu| = (0.05, 0.06)$ and $m_8/|\mu| = (0.07, 0.08)$ for the E order parameter (18). Here we don't show the numbers on the vertical axis⁶⁸ since only the position of LDOS peak can be probed in the STM experiments.

We would like to mention that if including the momentum dependence of the surface order parameter in each surface-mode region, it can broaden the LDOS peaks in Fig. 2. In addition, the momentum dependence may also lead to the existence of arcs of surface zero modes in certain small parameter regions as discussed Appendix E.

V. Impurity Effect

In this section, we will study the effect of surface non-magnetic and magnetic impurities. The effect of non-magnetic impurity on SMFBs in the absence of the mean-field order parameters has been studied in Ref. [55–57, and 69], showing that any non-magnetic impurity can generally induce a local gap for the SMFBs of DIII TNLS. Our work here aims to present a systematic study on how the LDOS of SMFBs is split around a single non-magnetic or magnetic impurity in the absence/presence of the mean-field order parameters.

A. Preliminaries

To consider the local potential, we first need to transform SMFBs to the real space with

$$b_{l_\chi, l_c, i, \mathbf{r}_\parallel}^\dagger = \frac{1}{\sqrt{S_\parallel}} \sum_{\mathbf{k}_\parallel} e^{-i\mathbf{k}_\parallel \cdot \mathbf{r}_\parallel} b_{i, \mathbf{k}_\parallel}^\dagger, \quad (21)$$

where the momentum summation is limited into the surface mode region A_{l_χ, l_c} . Under the symmetry operations, the indexes i, l_χ, l_c of $b_{l_\chi, l_c, i, \mathbf{r}_\parallel}^\dagger$ defined here are transformed in the same way as those of $b_{i, l_\chi, l_c}^\dagger$ defined in Sec. IV. In the following, we adopt the following approximation

$$\frac{1}{S_\parallel} \sum_{\mathbf{k}_\parallel} e^{i(\mathbf{k}_\parallel - \mathbf{K}_\parallel^{l_\chi, l_c}) \cdot \mathbf{r}_\parallel} \approx \delta^{(2)}(\mathbf{r}_\parallel), \quad (22)$$

resulting in

$$\{b_{l_\chi, l_c, i, \mathbf{r}_\parallel}^\dagger, b_{l'_\chi, l'_c, i', \mathbf{r}'_\parallel}\} = \delta_{l_\chi l'_\chi} \delta_{l_c l'_c} \delta_{ii'} \delta^{(2)}(\mathbf{r}_\parallel - \mathbf{r}'_\parallel). \quad (23)$$

Further, we define

$$d_{\mathbf{r}_\parallel}^\dagger = (b_{+,1,\mathbf{r}_\parallel}^\dagger, b_{+,2,\mathbf{r}_\parallel}^\dagger, b_{+,3,\mathbf{r}_\parallel}^\dagger, b_{-,1,\mathbf{r}_\parallel}^\dagger, b_{-,2,\mathbf{r}_\parallel}^\dagger, b_{-,3,\mathbf{r}_\parallel}^\dagger) \quad (24)$$

for convenience.

The behavior of $d_{\mathbf{r}_\parallel}^\dagger$ under the symmetry transformation is crucial for the understanding of LDOS. In general, the relation required by the PH symmetry has the form $d_{\mathbf{r}_\parallel}^\dagger \mathcal{C}_d = d_{\mathbf{r}_\parallel}^T$, and the transformation under TR, \hat{C}_3 , and $\hat{\Pi}$ operations reads $\hat{\mathcal{T}} d_{\mathbf{r}_\parallel}^\dagger \hat{\mathcal{T}}^{-1} = d_{\mathbf{r}_\parallel}^\dagger \mathcal{T}_d$, $\hat{C}_3 d_{\mathbf{r}_\parallel}^\dagger \hat{C}_3^{-1} = d_{\mathbf{r}_\parallel}^\dagger \mathcal{C}_{3,d}$, and $\hat{\Pi} d_{\mathbf{r}_\parallel}^\dagger \hat{\Pi}^{-1} = d_{\mathbf{r}_\parallel}^\dagger \Pi_d$, respectively. As $d_{\mathbf{r}_\parallel}^\dagger$, besides \mathbf{r}_\parallel , carries three indexes l_χ, l_c, i that transform independently under the symmetry operation, the transformation matrices presented above should be in the tensor product form as

$$\begin{aligned} \mathcal{C}_d &= \mathcal{C}_\chi \otimes \mathcal{C}_c \otimes \sigma_2 \text{ with } \mathcal{C}_\chi = -i\rho_2 \text{ and } \mathcal{C}_c = \lambda_0, \\ \mathcal{T}_d &= \mathcal{T}_\chi \otimes \mathcal{T}_c \otimes \mathcal{T}_b \text{ with } \mathcal{T}_\chi = \rho_1 \text{ and } \mathcal{T}_c = \lambda_0, \\ \mathcal{C}_{3,d} &= \mathcal{C}_{3,\chi} \otimes \mathcal{C}_{3,c} \otimes \mathcal{C}_{3,b} \text{ with } \mathcal{C}_{3,\chi} = \rho_0, \\ \Pi_d &= \Pi_\chi \otimes \Pi_c \otimes \Pi_b \text{ with } \Pi_\chi = \rho_0, \end{aligned} \quad (25)$$

where $\mathcal{C}_{3,c} = \exp(-i\frac{\lambda_2 - \lambda_5 + \lambda_7}{\sqrt{3}}\frac{2\pi}{3})$, $\Pi_c = -\exp(i\frac{\lambda_5 + \lambda_7}{\sqrt{2}}\pi)$, ρ_i 's are Pauli matrices for $l_\chi = \pm$ index, σ_i 's are for the pseudo-spin of the surface modes as before, and λ_i 's are Gell-Mann matrices (Appendix A) for $l_c = 1, 2, 3$ index with λ_0 the 3×3 identity matrix. In addition, the representation of the translation operator perpendicular to (111) direction is $\hat{T}_{\mathbf{x}_\parallel} d_{\mathbf{r}_\parallel}^\dagger \hat{T}_{\mathbf{x}_\parallel}^{-1} = d_{\mathbf{r}_\parallel + \mathbf{x}_\parallel}^\dagger$.

With the above definition of $d_{\mathbf{r}_\parallel}^\dagger$ operator, we next consider the Hamiltonian that describes the effect of a surface impurity on the SMFBs, given by

$$H_V = \int d^2 r_\parallel d_{\mathbf{r}_\parallel}^\dagger M_V(\mathbf{r}_\parallel) d_{\mathbf{r}_\parallel} + \text{const.}, \quad (26)$$

where $M_V(\mathbf{r}_\parallel)$ is Hermitian, the PH symmetry requires $\mathcal{C}_d M_V^*(\mathbf{r}_\parallel) \mathcal{C}_d^\dagger = -M_V(\mathbf{r}_\parallel)$, and the impurity is chosen to be at $\mathbf{r}_\parallel = 0$ without the loss of generality. Such form of impurity Hamiltonian is justified in Appendix.F. $M_V(\mathbf{r}_\parallel)$ in general is the linear combination of $\rho_j \otimes \lambda_k \otimes \sigma_l$ with coefficients depending on \mathbf{r}_\parallel . In this case, we can convert the symmetry transformation of l_χ and l_c indexes of $M_V(\mathbf{r}_\parallel)$ to the transformations of ρ_j 's and λ_k 's, respectively. Based on Eq. (25), ρ_j 's and λ_k 's can be classified according to the IRs of C_{3v} and parities of TR, PH and χ , as shown in the second lowest and lowest parts of Tab. I. Then, the terms in $M_V(\mathbf{r}_\parallel)$ with certain symmetry properties can be constructed via the tensor product of the classified ρ_j 's, λ_k 's and σ_l 's listed in Tab. I, which can further determine the number of LDOS peaks. Similar as Sec. IV, the LDOS discussed here is based on the full spectrum of $M_V(\mathbf{r}_\parallel)$, of which only the half with non-negative energy is physical. In the following, we study the LDOS at the impurity position $\mathbf{r}_\parallel = 0$ with the focus on two types of impurities: (i) non-magnetic charge impurity, and (ii) magnetic impurity with magnetization along the (111) direction.

B. Non-magnetic Charge Impurity

For a charge impurity, the potential term $M_V(\mathbf{r}_\parallel = 0) = M_c$ possesses the TR symmetry $\mathcal{T}_d M_c^* \mathcal{T}_d^\dagger = M_c$, the C_{3v} symmetries centered at the impurity $R_d M_c R_d^\dagger = M_c$ with $R \in C_{3v}$, and the chiral symmetry $\chi_d M_c \chi_d^\dagger = -M_c$. (See Appendix.F for details.) According to its symmetry properties and Tab. I, the generic form of M_c reads

$$\begin{aligned} M_c = & (\eta_1 \rho_1 + \eta_2 \rho_2) \otimes \Lambda_1 \otimes \sigma_0 \\ & + (\eta_3 \rho_1 + \eta_4 \rho_2) \otimes \Lambda_2 \otimes \sigma_0 + (\eta_5 \rho_1 + \eta_6 \rho_2) \otimes \Lambda_3 \otimes \sigma_3 \\ & + (\eta_7 \rho_1 + \eta_8 \rho_2) \otimes (-\Lambda_{5,1} \otimes \sigma_2 + \Lambda_{5,2} \otimes \sigma_1), \end{aligned} \quad (27)$$

where η_1, \dots, η_8 are real. Below we examine the LDOS on a single charge impurity for SMFBs and compare the case without any order parameter to the cases with A_1 (16), A_2 (17), and E (18) order parameters. The LDOS around the charge impurity is shown in Figs. 3a-d, which reveal the following features. (1) Since PH symmetry exists in all the cases, the LDOS is always symmetric with respect to zero energy. (2) If no order parameters exist, there are six peaks (Fig. 3a), given by the TR protected double degeneracy of each eigenvalue of M_c according to the Kramer's degeneracy. (3) In the presence of the A_1 order parameter, 8 peaks exist at the impurity (Fig. 3b). The reason is the following. Since the translational invariance is absent, the modes with different l_χ or l_c are coupled by the charge impurity, and the three-fold degeneracy for the pure A_1 order parameter case is lifted. Moreover, the appearance of the order parameter breaks the TR symmetry, leaving only the C_{3v} symmetries to protect the degeneracy. For convenience, we choose the eigenstates of \hat{C}_3 rotation as the bases to make the representation

$C_{3,d}$ diagonal as

$$\tilde{C}_{3,d} = \begin{pmatrix} e^{-i\frac{\pi}{3}} \mathbb{1}_4 & & \\ & -\mathbb{1}_4 & \\ & & e^{i\frac{\pi}{3}} \mathbb{1}_4 \end{pmatrix}, \quad (28)$$

where $\mathbb{1}_n$ is the $n \times n$ identity matrix. Due to the presence of the A_1 order parameter, the Hamiltonian at the charge impurity becomes $M_c + M_{A_1}$ with M_{A_1} given by transforming Eq. (16) to the d bases. (See Appendix.F.) With the eigen-bases of \hat{C}_3 rotation, $M_c + M_{A_1}$ can be block diagonalized as $\text{diag}(h_1, h_2, h_3)$, where h_1 , h_2 and h_3 are 4×4 Hermitian matrices. With the same bases, the mirror matrix Π_d has the form

$$\tilde{\Pi}_d = \begin{pmatrix} & U_\Pi \\ & U_\Pi \\ U_\Pi & \end{pmatrix} \quad (29)$$

with

$$U_\Pi = \begin{pmatrix} 0 & -1 & 0 & 0 \\ 1 & 0 & 0 & 0 \\ 0 & 0 & 0 & -1 \\ 0 & 0 & 1 & 0 \end{pmatrix}. \quad (30)$$

The mirror symmetry gives $U_\Pi h_3 U_\Pi^\dagger = h_1$ and $U_\Pi h_2 U_\Pi^\dagger = h_2$, which means the eigenvalues of h_1 are the same as those of h_3 . In fact, the representations of symmetry operations show that the bases of h_1 and h_3 belong to two dimensional IRs of C_{3v} while those of h_2 belong to one dimensional IRs of C_{3v} . Therefore, $M_c + M_{A_1}$ has four doubly degenerate and four single eigenvalues, resulting in the 8 LDOS peaks. (4) The 12 LDOS peaks exist at the impurity in the presence of the A_2 order parameter (Fig. 3c) since the translational invariance and the odd mirror parity of the A_2 order parameter are broken by impurity, and there are no symmetries ensuring any degeneracy. (5) The 12 LDOS peaks at the impurity for the E order parameter (Fig. 3d) are because no new symmetries are brought by the impurity. Besides the above five features, the sign change of the charge does not affect the LDOS peaks since the order parameters are all chiral anti-symmetric while the charge impurity is chiral symmetric.

C. Magnetic Impurity

$M_V(\mathbf{r}_\parallel = 0) = M_m$ is still Hermitian and PH symmetric at a magnetic impurity with magnetic momentum along (111) direction. Moreover, it is TR-odd $\mathcal{T}_d M_m^* \mathcal{T}_d^\dagger = -M_m$, \hat{C}_3 -symmetric $C_{3,d} M_m C_{3,d}^\dagger = M_m$, and $\hat{\Pi}$ -odd $\Pi_d M_m \Pi_d^\dagger = -M_m$. (Appendix.F.) According

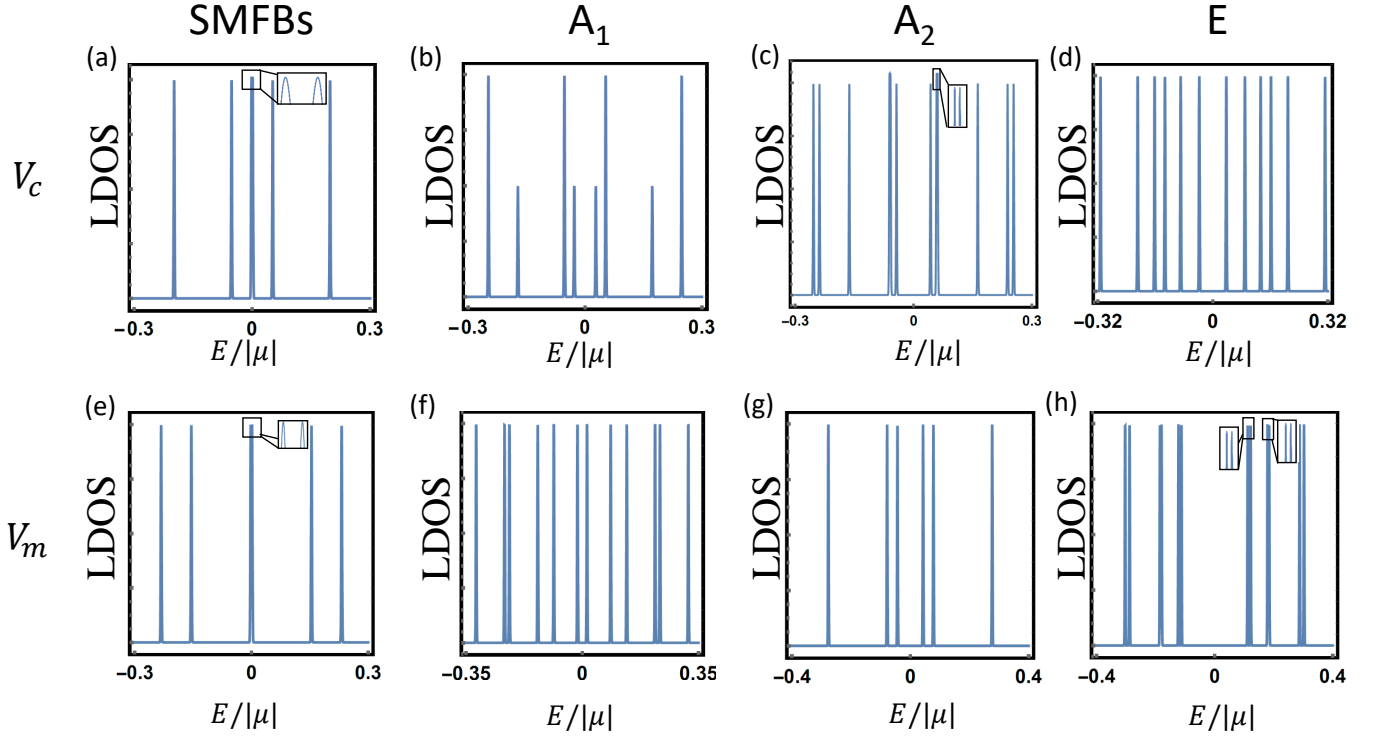


FIG. 3. The LDOS as a function of the energy ($E/|\mu|$) with surface impurities. The two rows from top to bottom are at a surface charge impurity and at a surface magnetic impurity, respectively. The four columns from left to right correspond to no order parameters, A_1 order parameter, A_2 order parameter and E order parameter, respectively. The broadening of each peak and the parameters choices for the orders if exist are the same as Fig. 2. The potential form of the charge or magnetic impurity is shown in Appendix F. The numbers on the vertical axes are again omitted.

to the symmetry properties and Tab. I, the generic form of M_m reads

$$\begin{aligned}
 M_m = & \eta_9 \rho_0 \otimes \Lambda_1 \otimes \sigma_3 \\
 & + \eta_{10} \rho_0 \otimes \Lambda_2 \otimes \sigma_3 + \eta_{11} \rho_0 \otimes \Lambda_3 \otimes \sigma_0 \\
 & + \eta_{12} \rho_0 \otimes (\Lambda_{4,2} \otimes \sigma_2 + \Lambda_{4,1} \otimes \sigma_1) \\
 & + \eta_{13} \rho_3 \otimes (\Lambda_{5,2} \otimes \sigma_2 + \Lambda_{5,1} \otimes \sigma_1) \\
 & + \eta_{14} \rho_0 \otimes (\Lambda_{6,2} \otimes \sigma_2 + \Lambda_{6,1} \otimes \sigma_1), \quad (31)
 \end{aligned}$$

where $\eta_{9,\dots,14}$ are real. Figs. 3e-h show the LDOS around the magnetic impurity and reveal the following features. (1) PH symmetry again ensures that the LDOS is always symmetric with respect to zero energy and the E order parameter still has 12 LDOS peaks at the magnetic impurity since no new symmetries appear as shown in Fig. 3h. (2) If no order parameters exist, there are six peaks (Figs. 3e), resulted from the double degeneracy given by the combination of the PH symmetry and odd $\hat{\Pi}$ parity. It is because the combination of the PH symmetry and odd $\hat{\Pi}$ parity gives $\Pi_d C_d M_m C_d^\dagger \Pi_d^\dagger = M_m$, and since $\Pi_d C_d (\Pi_d C_d)^* = -1$, each eigenvalue of M_m must be doubly degenerate (similar to Kramer's theorem). (3) The original 4 peaks of the A_1 order are splitted into 12 peaks since the magnetic impurity breaks the translational invariance and $\hat{\Pi}$ symmetry (Fig. 3f). (4) As shown in Fig. 3g, the 6 LDOS peaks of the magnetic impurity remain in the presence of the A_2 order since

the PH symmetry and odd $\hat{\Pi}$ parity are not broken. Besides the above four features, flipping the direction of the magnetic moment, i.e. $M_m \rightarrow -M_m$, does not affect the LDOS distribution in presence of the A_1 order parameter, since the A_1 order parameter has $\hat{\Pi}$ symmetry while M_m has odd $\hat{\Pi}$ parity.

D. Summary for Impurity Effect

To sum up, the number of LDOS peaks at a charge impurity or a magnetic impurity with magnetic moment in (111) direction is 6 or 6 for no order parameters, 8 or 12 for the A_1 order parameter, 12 or 6 for the A_2 order parameter, and 12 or 12 for the E order parameter, respectively, as summarized in Fig. 4. Combining the above results with the LDOS peaks without impurity given in Sec. IV, it is more than enough to identify the order parameters in our system. In the above analysis, we adopt the approximation (22), only consider translationally invariant order parameters that are \mathbf{k}_\parallel -independent in each surface mode region, and assume the surface mode wavefunctions are \mathbf{k}_\parallel -independent in each surface mode region to deal with the impurity. Those approximations neglect high-order effects which typically can only broaden the LDOS peaks without affecting the qualitative result.

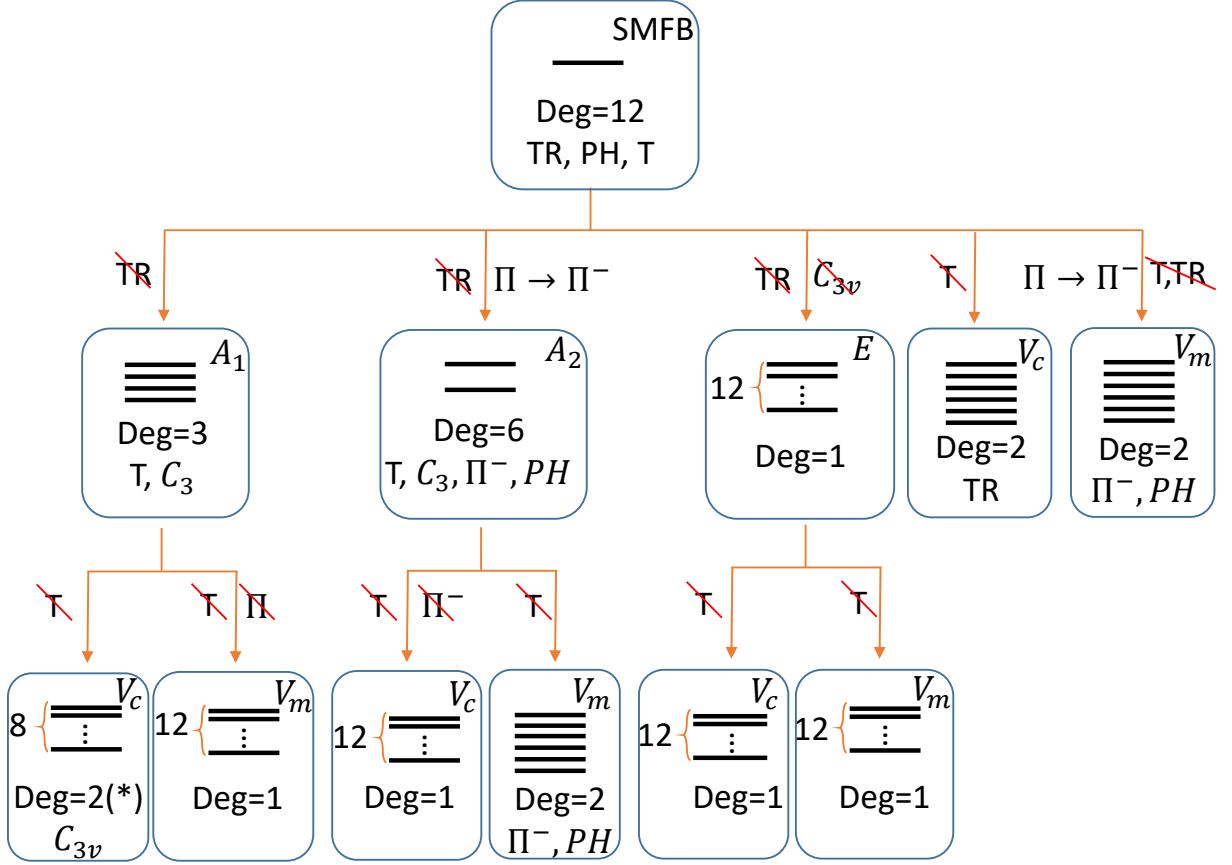


FIG. 4. This graph shows how the number of LDOS peaks shown in Fig. 2,3 is determined by the symmetry. The solid black lines indicate the LDOS peaks. A_1 , A_2 and E stand for the surface order parameters, and V_c and V_m denote the charge and magnetic impurity, respectively. “Deg” indicates the symmetry protected degeneracy of the each LDOS peak, except the case marked by (*) where only half of the eight peaks have the double degeneracy. If $Deg > 1$, the line below shows the crucial symmetries that account for the degeneracy. Here Π^- means odd mirror parity, T means the translational invariance, and the origin for the rotation C_3 or mirror Π is located at the impurity center. The red lines crossing the symmetry operations indicate the breaking of the corresponding symmetries.

VI. Conclusion and Discussion

In this work, we studied the energy spectrum (or LDOS) of the SMFBs localized on (111) surface of the half-Heusler SCs with translationally invariant order parameters or magnetic/non-magnetic impurities based on the Luttinger model with singlet-quintet mixing. Our work demonstrates that the zero-bias peak of SMFBs can be split to reveal a rich peak structure when different types of order parameters induced by interaction or magnetic/non-magnetic impurities are introduced. Such peak structure can be viewed as a fingerprint to distinguish different types of order parameters in the standard STM experiments. In addition, we notice that the SMFBs induced by singlet-septet mixing proposed in Ref. [34] possess six patches without any additional pseudospin degeneracy in the surface Brillouin zone (see Fig. 5a and the discussion in Ref. [39]). Due to the dif-

ferent number of degeneracy, we expect the peak structures given by the order parameters and magnetic/non-magnetic impurities will be different in two cases, which thereby may help distinguish the singlet-quintet mixing from the singlet-septet mixing in experiments.

VII. Acknowledgement

We acknowledge the helpful discussion with C.Wu. J.Y thanks Yang Ge, Rui-Xing Zhang, Jian-Xiao Zhang and Tongzhou Zhao for helpful discussion. We acknowledge the support of the Office of Naval Research (Grant No. N00014-18-1-2793), Kaufman New Initiative research grant KA2018-98553 of the Pittsburgh Foundation and the U.S. Department of Energy (Grant No. DESC0019064).

Appendix A Convention and Expressions

The Fourier transformation of creation operators in the continuous limit reads

$$c_{\mathbf{r}}^\dagger = \frac{1}{\sqrt{\mathcal{V}}} \sum_{\mathbf{k}} e^{-i\mathbf{k}\cdot\mathbf{r}} c_{\mathbf{k}}^\dagger, \quad (32)$$

where \mathcal{V} is the total volume of the entire space.

The five d-orbital cubic harmonics read⁷⁰

$$\begin{cases} g_{\mathbf{k},1} = \sqrt{3}k_y k_z \\ g_{\mathbf{k},2} = \sqrt{3}k_z k_x \\ g_{\mathbf{k},3} = \sqrt{3}k_x k_y \\ g_{\mathbf{k},4} = \frac{\sqrt{3}}{2}(k_x^2 - k_y^2) \\ g_{\mathbf{k},5} = \frac{1}{2}(2k_z^2 - k_x^2 - k_y^2) \end{cases}. \quad (33)$$

The $j = \frac{3}{2}$ angular momentum matrices are⁵⁹

$$J_x = \begin{pmatrix} 0 & \frac{\sqrt{3}}{2} & 0 & 0 \\ \frac{\sqrt{3}}{2} & 0 & 1 & 0 \\ 0 & 1 & 0 & \frac{\sqrt{3}}{2} \\ 0 & 0 & \frac{\sqrt{3}}{2} & 0 \end{pmatrix} \quad (34)$$

$$J_y = \begin{pmatrix} 0 & -\frac{i\sqrt{3}}{2} & 0 & 0 \\ \frac{i\sqrt{3}}{2} & 0 & -i & 0 \\ 0 & i & 0 & -\frac{i\sqrt{3}}{2} \\ 0 & 0 & \frac{i\sqrt{3}}{2} & 0 \end{pmatrix} \quad (35)$$

$$J_z = \begin{pmatrix} \frac{3}{2} & 0 & 0 & 0 \\ 0 & \frac{1}{2} & 0 & 0 \\ 0 & 0 & -\frac{1}{2} & 0 \\ 0 & 0 & 0 & -\frac{3}{2} \end{pmatrix}. \quad (36)$$

The five Gamma matrices are⁷⁰

$$\begin{cases} \Gamma^1 = \frac{1}{\sqrt{3}}(J_y J_z + J_z J_y) \\ \Gamma^2 = \frac{1}{\sqrt{3}}(J_z J_x + J_x J_z) \\ \Gamma^3 = \frac{1}{\sqrt{3}}(J_x J_y + J_y J_x) \\ \Gamma^4 = \frac{1}{\sqrt{3}}(J_x^2 - J_y^2) \\ \Gamma^5 = \frac{1}{3}(2J_z^2 - J_x^2 - J_y^2) \end{cases}. \quad (37)$$

Clearly, $\{\Gamma^a, \Gamma^b\} = 2\delta_{ab}\Gamma^0$ where Γ^0 is the 4 by 4 identity matrix.

C_{3v}	$\mathbb{1}$	C_3	Π
A_1	1	1	1
A_2	1	1	-1
E	2	-1	0

TABLE II. Character table of C_{3v} . Here $\mathbb{1}$ means identity operation.⁷¹

C_{3v}		TR
A_1	$n_0 = \Gamma_0$	+
A_1	$n_1 = \frac{1}{\sqrt{3}}(\Gamma_1 + \Gamma_2 + \Gamma_3)$	+
A_1	$n_2 = \frac{1}{\sqrt{3}}(V_x + V_y + V_z)$	-
A_2	$n_3 = J_{xyz}$	-
A_2	$n_4 = \frac{1}{\sqrt{3}}(J_x + J_y + J_z)$	-
A_2	$n_5 = \frac{1}{\sqrt{3}}(P_x + P_y + P_z)$	-
E	$\mathbf{n}_6 = (\frac{1}{\sqrt{6}}(\Gamma_1 + \Gamma_2 - 2\Gamma_3), \frac{1}{\sqrt{2}}(-\Gamma_1 + \Gamma_2))$	+
E	$\mathbf{n}_7 = (\Gamma_5, \Gamma_4)$	+
E	$\mathbf{n}_8 = (\frac{1}{\sqrt{2}}(J_x - J_y), \frac{1}{\sqrt{6}}(J_x + J_y - 2J_z))$	-
E	$\mathbf{n}_9 = (\frac{1}{\sqrt{2}}(P_x - P_y), \frac{1}{\sqrt{6}}(P_x + P_y - 2P_z))$	-
E	$\mathbf{n}_{10} = (\frac{1}{\sqrt{6}}(V_x + V_y - 2V_z), \frac{1}{\sqrt{2}}(-V_x + V_y))$	-

TABLE III. Expressions of n_i in Eq. (14). $P_i = J_i^3 - 41J_i/20$, $V_x = \frac{1}{2}\{J_x, J_y^2 - J_z^2\}$, $V_y = \frac{1}{2}\{J_y, J_z^2 - J_x^2\}$, $V_z = \frac{1}{2}\{J_z, J_x^2 - J_y^2\}$ and $J_{xyz} = J_x J_y J_z + J_z J_y J_x$.

C_{3v}		TR
A_1	$N_1(\mathbf{k}_{ }) = \delta_{\mathbf{k}_{ }}^\chi \sigma_0$	-
A_1	$N_2(\mathbf{k}_{ }) = \delta_{\mathbf{k}_{ }}^{E_1,+}(-\sigma_2) + \delta_{\mathbf{k}_{ }}^{E_2,+} \sigma_1$	-
A_2	$N_3(\mathbf{k}_{ }) = \sigma_3$	-
A_2	$N_4(\mathbf{k}_{ }) = -\delta_{\mathbf{k}_{ }}^{E_2,+}(-\sigma_2) + \delta_{\mathbf{k}_{ }}^{E_1,+} \sigma_1$	-
E	$\mathbf{N}_5(\mathbf{k}_{ }) = (\delta_{\mathbf{k}_{ }}^{E_1,-} \sigma_0, \delta_{\mathbf{k}_{ }}^{E_2,-} \sigma_0)$	-
E	$\mathbf{N}_6(\mathbf{k}_{ }) = (-\delta_{\mathbf{k}_{ }}^{E_2,+} \sigma_3, \delta_{\mathbf{k}_{ }}^{E_1,+} \sigma_3)$	-
E	$\mathbf{N}_7(\mathbf{k}_{ }) = (-\sigma_2, \sigma_1)$	-
E	$\mathbf{N}_8(\mathbf{k}_{ }) = (-\delta_{\mathbf{k}_{ }}^{E_1,+}(-\sigma_2) + \delta_{\mathbf{k}_{ }}^{E_2,+} \sigma_1, \delta_{\mathbf{k}_{ }}^{E_1,+} \sigma_1 + \delta_{\mathbf{k}_{ }}^{E_2,+}(-\sigma_2))$	-

TABLE IV. Expressions of N_i in Eq. (16), Eq. (17) and Eq. (18).

The list of Gell-Mann matrices⁷²

$$\begin{aligned}
\lambda_1 &= \begin{pmatrix} 0 & 1 & 0 \\ 1 & 0 & 0 \\ 0 & 0 & 0 \end{pmatrix} & \lambda_2 &= \begin{pmatrix} 0 & -i & 0 \\ i & 0 & 0 \\ 0 & 0 & 0 \end{pmatrix} \\
\lambda_3 &= \begin{pmatrix} 1 & 0 & 0 \\ 0 & -1 & 0 \\ 0 & 0 & 0 \end{pmatrix} & \lambda_4 &= \begin{pmatrix} 0 & 0 & 1 \\ 0 & 0 & 0 \\ 1 & 0 & 0 \end{pmatrix} \\
\lambda_5 &= \begin{pmatrix} 0 & 0 & -i \\ 0 & 0 & 0 \\ i & 0 & 0 \end{pmatrix} & \lambda_6 &= \begin{pmatrix} 0 & 0 & 0 \\ 0 & 0 & 1 \\ 0 & 1 & 0 \end{pmatrix} \\
\lambda_7 &= \begin{pmatrix} 0 & 0 & 0 \\ 0 & 0 & -i \\ 0 & i & 0 \end{pmatrix} & \lambda_8 &= \frac{1}{\sqrt{3}} \begin{pmatrix} 1 & 0 & 0 \\ 0 & 1 & 0 \\ 0 & 0 & -2 \end{pmatrix}
\end{aligned} \quad (38)$$

And λ_0 is defined as the 3×3 identity matrix.

Appendix B Representations of Symmetry Operators

In this section, we show the representation of symmetry operators on the $c_{\mathbf{k}}$ bases and the Nambu bases. Before showing the representation, we define the following notations: \hat{P}_F is the fermion parity operator, $\hat{T}_{\mathbf{x}}$ with $\mathbf{x} \in \mathbb{R}^3$ is a generic translation operator, the generators of O_h group \hat{C}_3 , \hat{P} , \hat{C}_4 and $\hat{\Pi}$ are 3-fold rotations along (111), inversion, 4-fold rotation along (001) and mirror perpendicular to (110), respectively, and $\hat{\mathcal{T}}$ is the time-reversal operator. Representations of $O(3)$ are not shown here since we only care about the $c_1 \neq c_2$ case.

1 The $c_{\mathbf{k}}$ Bases

$$\hat{P}_F c_{\mathbf{k}}^\dagger \hat{P}_F^{-1} = -c_{\mathbf{k}}^\dagger, \quad \hat{P}_F c_{\mathbf{k}} \hat{P}_F^{-1} = -c_{\mathbf{k}}, \quad (39)$$

$$\hat{T}_{\mathbf{x}} c_{\mathbf{k}}^\dagger \hat{T}_{\mathbf{x}}^{-1} = e^{-i\mathbf{k} \cdot \mathbf{x}} c_{\mathbf{k}}^\dagger, \quad \hat{T}_{\mathbf{x}} c_{\mathbf{k}} \hat{T}_{\mathbf{x}}^{-1} = e^{i\mathbf{k} \cdot \mathbf{x}} c_{\mathbf{k}}, \quad (40)$$

$$\hat{C}_3 c_{\mathbf{k}}^\dagger \hat{C}_3^{-1} = c_{C_3 \mathbf{k}}^\dagger, \quad \hat{C}_3 c_{\mathbf{k}} \hat{C}_3^{-1} = c_{C_3 \mathbf{k}}, \quad (41)$$

$$\hat{P} c_{\mathbf{k}}^\dagger \hat{P}^{-1} = -c_{-\mathbf{k}}^\dagger, \quad \hat{P} c_{\mathbf{k}} \hat{P}^{-1} = -c_{-\mathbf{k}}, \quad (42)$$

$$\hat{C}_4 c_{\mathbf{k}}^\dagger \hat{C}_4^{-1} = c_{C_4 \mathbf{k}}^\dagger, \quad \hat{C}_4 c_{\mathbf{k}} \hat{C}_4^{-1} = c_{C_4 \mathbf{k}}, \quad (43)$$

$$\hat{\Pi} c_{\mathbf{k}}^\dagger \hat{\Pi}^{-1} = c_{\Pi \mathbf{k}}^\dagger, \quad \hat{\Pi} c_{\mathbf{k}} \hat{\Pi}^{-1} = c_{\Pi \mathbf{k}}, \quad (44)$$

$$\hat{\mathcal{T}} c_{\mathbf{k}}^\dagger \hat{\mathcal{T}}^{-1} = c_{-\mathbf{k}}^\dagger \gamma, \quad \hat{\mathcal{T}} c_{\mathbf{k}} \hat{\mathcal{T}}^{-1} = \gamma^\dagger c_{-\mathbf{k}}, \quad (45)$$

where $C_3 = \exp(-i \frac{J_x + J_y + J_z}{\sqrt{3}} \frac{2\pi}{3})$, $C_3 \mathbf{k} = (k_z, k_x, k_y)$, $C_4 = \exp(-i J_z \frac{2\pi}{4})$, $C_4 \mathbf{k} = (-k_y, k_x, k_z)$, $\Pi = -\exp(-i \frac{J_x - J_y}{\sqrt{2}} \frac{2\pi}{2})$ and $\Pi \mathbf{k} = (k_y, k_x, k_z)$.

2 The Nambu Bases

$$\hat{P}_F \Psi_{\mathbf{k}}^\dagger \hat{P}_F^{-1} = -\Psi_{\mathbf{k}}^\dagger, \quad \hat{P}_F \Psi_{\mathbf{k}} \hat{P}_F^{-1} = -\Psi_{\mathbf{k}}, \quad (46)$$

$$\hat{T}_{\mathbf{x}} \Psi_{\mathbf{k}}^\dagger \hat{T}_{\mathbf{x}}^{-1} = e^{-i\mathbf{k} \cdot \mathbf{x}} \Psi_{\mathbf{k}}^\dagger, \quad \hat{T}_{\mathbf{x}} \Psi_{\mathbf{k}} \hat{T}_{\mathbf{x}}^{-1} = e^{i\mathbf{k} \cdot \mathbf{x}} \Psi_{\mathbf{k}}, \quad (47)$$

$$\hat{C}_3 \Psi_{\mathbf{k}}^\dagger \hat{C}_3^{-1} = \Psi_{C_3 \mathbf{k}}^\dagger, \quad \hat{C}_3 \Psi_{\mathbf{k}} \hat{C}_3^{-1} = \Psi_{C_3 \mathbf{k}}, \quad (48)$$

$$\hat{P} \Psi_{\mathbf{k}}^\dagger \hat{P}^{-1} = -\Psi_{-\mathbf{k}}^\dagger, \quad \hat{P} \Psi_{\mathbf{k}} \hat{P}^{-1} = -\Psi_{-\mathbf{k}}, \quad (49)$$

$$\hat{C}_4 \Psi_{\mathbf{k}}^\dagger \hat{C}_4^{-1} = \Psi_{C_4 \mathbf{k}}^\dagger, \quad \hat{C}_4 \Psi_{\mathbf{k}} \hat{C}_4^{-1} = \Psi_{C_4 \mathbf{k}}, \quad (50)$$

$$\hat{\Pi} \Psi_{\mathbf{k}}^\dagger \hat{\Pi}^{-1} = \Psi_{\Pi \mathbf{k}}^\dagger, \quad \hat{\Pi} \Psi_{\mathbf{k}} \hat{\Pi}^{-1} = \Psi_{\Pi \mathbf{k}}, \quad (51)$$

$$\hat{\mathcal{T}} \Psi_{\mathbf{k}}^\dagger \hat{\mathcal{T}}^{-1} = \Psi_{-\mathbf{k}}^\dagger \mathcal{T}, \quad \hat{\mathcal{T}} \Psi_{\mathbf{k}} \hat{\mathcal{T}}^{-1} = \mathcal{T}^\dagger \Psi_{-\mathbf{k}}, \quad (52)$$

where $\tilde{C}_3 = \text{diag}(C_3, C_3^*)$, $\tilde{C}_4 = \text{diag}(C_4, C_4^*)$, $\tilde{\Pi} = \text{diag}(\Pi, \Pi^*)$ and $\mathcal{T} = \text{diag}(\gamma, \gamma^*)$. \tilde{C}_3 , $\tilde{\Pi}$, $\mathcal{T}K$ and $\mathcal{C}K$ commute with each other, where K is the complex conjugate operation. χ anti-commutes with $\mathcal{T}K$ and $\mathcal{C}K$ and commutes with \tilde{C}_3 and $\tilde{\Pi}$.

Appendix C Surface Majorana Flat Bands

1 Existence of Surface Zero Modes

Due to the topological invariant $N_w = \pm 2$ at each non-trivial $\mathbf{k}_{||}$, we expect two boundary modes at each non-trivial $\mathbf{k}_{||}$ on one surface of our model.⁴⁰ Therefore, we consider a semi-infinite version of Eq. (1) ($x_{\perp} < 0$) with open boundary condition at $x_{\perp} = 0$, where x_{\perp} is the position on (111) axis. The corresponding Hamiltonian reads

$$\begin{aligned}
H_{\perp} &= \frac{1}{2} \sum_{\mathbf{k}_{||}} \int_{-\infty}^0 dx_{\perp} \Psi_{\mathbf{k}_{||}, x_{\perp}}^\dagger h_{BdG}(\mathbf{k}_{||}, -i\partial_{x_{\perp}}) \Psi_{\mathbf{k}_{||}, x_{\perp}} \\
&+ \sum_{\mathbf{k}_{||}} \int_0^{+\infty} dx_{\perp} E_{\infty} c_{\mathbf{k}_{||}, x_{\perp}}^\dagger c_{\mathbf{k}_{||}, x_{\perp}} + \text{const.}, \quad (53)
\end{aligned}$$

where $c_{\mathbf{k}_{||}, x_{\perp}}^\dagger = \frac{1}{\sqrt{L_{\perp}}} \sum_{\mathbf{k}_{\perp}} e^{-i\mathbf{k}_{\perp} \cdot \mathbf{x}_{\perp}} c_{\mathbf{k}}^\dagger$ with L_{\perp} the length along the (111) direction of the entire space,

$h_{BdG}(\mathbf{k}_{||}, -i\partial_{x_{\perp}})$ is obtained by replacing k_{\perp} in $h_{BdG}(\mathbf{k})$ by $-i\partial_{x_{\perp}}$, $\Psi_{\mathbf{k}_{||}, x_{\perp}}^{\dagger} = (c_{\mathbf{k}_{||}, x_{\perp}}^{\dagger}, c_{-\mathbf{k}_{||}, x_{\perp}}^T)$, and $E_{\infty} \rightarrow +\infty$ is for the open boundary condition. For such a semi-infinite system, the translation symmetry in the (111) direction, the inversion symmetry and the 4-fold rotational symmetry along (001) are broken. The Hamiltonian $h_{BdG}(\mathbf{k}_{||}, -i\partial_{x_{\perp}})$ still has PH, TR, chiral and C_{3v} symmetries $-\mathcal{C}[h_{BdG}(-\mathbf{k}_{||}, -i\partial_{x_{\perp}})]^* \mathcal{C}^{\dagger} = h_{BdG}(\mathbf{k}_{||}, -i\partial_{x_{\perp}})$, $\mathcal{T}[h_{BdG}(-\mathbf{k}_{||}, -i\partial_{x_{\perp}})]^* \mathcal{T}^{\dagger} = h_{BdG}(\mathbf{k}_{||}, -i\partial_{x_{\perp}})$, $-\chi h_{BdG}(\mathbf{k}_{||}, -i\partial_{x_{\perp}}) \chi^{\dagger} = h_{BdG}(\mathbf{k}_{||}, -i\partial_{x_{\perp}})$ and $\tilde{R} h_{BdG}(R^{-1} \mathbf{k}_{||}, -i\partial_{x_{\perp}}) \tilde{R}^{\dagger} = h_{BdG}(\mathbf{k}_{||}, -i\partial_{x_{\perp}})$, respectively, where $R = C_3, \Pi$. In addition, the PH symmetry requires $\mathcal{C}(\Psi_{-\mathbf{k}_{||}, x_{\perp}}^{\dagger})^T = \Psi_{\mathbf{k}_{||}, x_{\perp}}$ and the commutation relation is

$$\{\Psi_{\mathbf{k}_{||}, x_{\perp}, \alpha, s}^{\dagger}, \Psi_{\mathbf{k}'_{||}, x'_{\perp}, \alpha', s'}\} = \delta_{\mathbf{k}_{||}, \mathbf{k}'_{||}} \delta(x_{\perp} - x'_{\perp}) \delta_{\alpha\alpha'} \delta_{ss'} \quad (54)$$

$$\{\Psi_{\mathbf{k}_{||}, x_{\perp}, \alpha, s}^{\dagger}, \Psi_{\mathbf{k}'_{||}, x'_{\perp}, \alpha', s'}\} = \delta_{\mathbf{k}_{||}, -\mathbf{k}'_{||}} \delta(x_{\perp} - x'_{\perp}) (\tau_x)_{\alpha\alpha'} \delta_{ss'},$$

where $\alpha, \alpha' = 1, 2$ stand for the particle-hole index and s, s' are spin index of the $j = 3/2$ fermion.

The surface mode with zero energy $b_{\mathbf{k}_{||}}^{\dagger}$ of H_{\perp} in Eq. (53) is defined as

$$b_{\mathbf{k}_{||}}^{\dagger} = \int_{-\infty}^0 dx_{\perp} \Psi_{\mathbf{k}_{||}, x_{\perp}}^{\dagger} v_{\mathbf{k}_{||}, x_{\perp}}, \quad (55)$$

which satisfies $[H_{\perp}, b_{\mathbf{k}_{||}}^{\dagger}] = 0$ and $v_{\mathbf{k}_{||}, 0} = v_{\mathbf{k}_{||}, -\infty} = 0$. With the PH symmetry and the commutation relation, the equation $[H_{\perp}, b_{\mathbf{k}_{||}}^{\dagger}] = 0$ can be simplified as

$$h_{BdG}(\mathbf{k}_{||}, -i\partial_{x_{\perp}}) v_{\mathbf{k}_{||}, x_{\perp}} = 0. \quad (56)$$

Now we try to figure out the properties of the solution. First, transform the above equation to chiral eigen-bases:

$$U_{\chi}^{\dagger} h_{BdG}(\mathbf{k}_{||}, -i\partial_{x_{\perp}}) U_{\chi} U_{\chi}^{\dagger} v_{\mathbf{k}_{||}, x_{\perp}} = 0, \quad (57)$$

where

$$U_{\chi} = \frac{1}{\sqrt{2}} \begin{pmatrix} \mathbb{1}_4 & \mathbb{1}_4 \\ i\gamma & -i\gamma \end{pmatrix} \quad (58)$$

is the unitary matrix that diagonalizes χ :

$$U_{\chi}^{\dagger} \chi U_{\chi} = \begin{pmatrix} \mathbb{1}_4 & \\ & -\mathbb{1}_4 \end{pmatrix} \quad (59)$$

,

$$U_{\chi}^{\dagger} h_{BdG}(\mathbf{k}_{||}, -i\partial_{x_{\perp}}) U_{\chi} = \begin{pmatrix} & q(\mathbf{k}_{||}, -i\partial_{x_{\perp}}) \\ [q(\mathbf{k}_{||}, i\partial_{x_{\perp}})]^{\dagger} & \end{pmatrix}, \quad (60)$$

and

$$q(\mathbf{k}_{||}, -i\partial_{x_{\perp}}) = h(\mathbf{k}_{||}, -i\partial_{x_{\perp}}) - i\Delta(\mathbf{k}_{||}, -i\partial_{x_{\perp}}) \gamma. \quad (61)$$

The TR and PH matrices in the chiral representation read

$$U_{\chi}^{\dagger} \mathcal{T} U_{\chi}^* = \begin{pmatrix} & \gamma \\ \gamma & \end{pmatrix} \quad (62)$$

and

$$U_{\chi}^{\dagger} \mathcal{C} U_{\chi}^* = \begin{pmatrix} & i\gamma \\ -i\gamma & \end{pmatrix}. \quad (63)$$

In the chiral representation, both TR and PH symmetries give the same condition on q :

$$\gamma[q(-\mathbf{k}_{||}, i\partial_{x_{\perp}})]^T \gamma^{\dagger} = q(\mathbf{k}_{||}, -i\partial_{x_{\perp}}). \quad (64)$$

By defining $U_{\chi}^{\dagger} v_{\mathbf{k}_{||}, x_{\perp}} = (u_{\mathbf{k}_{||}, x_{\perp}}^T, w_{\mathbf{k}_{||}, x_{\perp}}^T)^T$ with $u(w)$ corresponding to chiral eigen-wavefunction with chiral eigenvalues $1(-1)$, Eq. (57) can be expressed as

$$\begin{cases} q(\mathbf{k}_{||}, -i\partial_{x_{\perp}}) w_{\mathbf{k}_{||}, x_{\perp}} = 0 \\ q^{\dagger}(\mathbf{k}_{||}, -i\partial_{x_{\perp}}) u_{\mathbf{k}_{||}, x_{\perp}} = 0 \end{cases}. \quad (65)$$

Since $h_{BdG}(-\mathbf{k}_{||}, i\partial_{x_{\perp}}) = h_{BdG}(\mathbf{k}_{||}, -i\partial_{x_{\perp}})$ originated from the bulk inversion symmetry, we have $q(\mathbf{k}_{||}, -i\partial_{x_{\perp}}) = q(-\mathbf{k}_{||}, i\partial_{x_{\perp}})$. Combined with TR, the equation of u in Eq. (65) can be transformed to

$$q(\mathbf{k}_{||}, -i\partial_{x_{\perp}}) \gamma^T u_{\mathbf{k}_{||}, -x_{\perp}}^* = 0. \quad (66)$$

Since $u_{\mathbf{k}_{||}, x_{\perp}} = 0$ for $x_{\perp} = 0, -\infty$ which means $\gamma^T u_{\mathbf{k}_{||}, -x_{\perp}}^* = 0$ for $x_{\perp} = 0, +\infty$, the above equation is the same as the equation of w except that the open boundary conditions are at $x_{\perp} = 0, +\infty$. Therefore, we can solve the equation of w in Eq. (65), i.e.

$$q(\mathbf{k}_{||}, -i\partial_{x_{\perp}}) w_{\mathbf{k}_{||}, x_{\perp}} = 0, \quad (67)$$

with $w_{\mathbf{k}_{||}, 0} = w_{\mathbf{k}_{||}, -\infty} = 0$ to have the solutions of w and with $w_{\mathbf{k}_{||}, 0} = w_{\mathbf{k}_{||}, \infty} = 0$ to have the solutions of u by $u_{\mathbf{k}_{||}, x_{\perp}} = \gamma w_{\mathbf{k}_{||}, -x_{\perp}}^*$.

With the ansatz $w_{\mathbf{k}_{||}, x_{\perp}} = e^{\lambda x_{\perp}} \bar{w}_{\mathbf{k}_{||}}$, the Eq. (67) becomes

$$q(\mathbf{k}_{||}, -i\lambda) \bar{w}_{\mathbf{k}_{||}} = 0 \quad (68)$$

with the solution determined by the octic equation $\det[q(\mathbf{k}_{||}, -i\lambda)] = 0$ for λ . The equation has 4 double roots $\lambda_{1,2,3,4}$ since $\det[q(\mathbf{k}_{||}, -i\lambda)]$ can be written in the form of the square of certain function, $\det[q(\mathbf{k}_{||}, -i\lambda)] = [\tilde{q}(\mathbf{k}_{||}, -i\lambda)]^2$.⁴⁰ In addition, since $\tilde{q}(\mathbf{k}_{||}, -i\lambda)$ does not have λ^3 term, the sum of $\lambda_{1,2,3,4}$ is zero. Each double root λ_i can give two orthogonal solutions $\bar{w}_{\mathbf{k}_{||}, i, j}$ of Eq. (68) with $i = 1, 2, 3, 4$ and $j = 1, 2$. Then the general solution of Eq. (67) without boundary condition reads

$$w_{\mathbf{k}_{||}, x_{\perp}} = \sum_{i=1}^4 \sum_{j=1}^2 b_{ij} e^{\lambda_i x_{\perp}} \bar{w}_{\mathbf{k}_{||}, i, j}. \quad (69)$$

Now let us impose the boundary condition. $w_{\mathbf{k}_\parallel, \infty} = 0$ or $w_{\mathbf{k}_\parallel, -\infty} = 0$ requires $Re[\lambda_i] < 0$ or $Re[\lambda_i] > 0$, respectively, and $w_{\mathbf{k}_\parallel, 0} = 0$ requires $\sum_{i,j} b_{ij} \bar{w}_{\mathbf{k}_\parallel, i, j} = 0$. Since the sum of the four λ_i 's is zero, it is impossible to have four $Re[\lambda_i]$'s with the same sign. If only two $Re[\lambda_i]$'s have the same sign, there will be typically no solutions, since the corresponding four four-component $\bar{w}_{\mathbf{k}_\parallel, i, j}$'s typically can not be linearly dependent. If three λ_i 's satisfy $Re[\lambda_i] > 0 (Re[\lambda_i] < 0)$, there are six corresponding four-component $\bar{w}_{\mathbf{k}_\parallel, i, j}$'s, resulting in two solutions to $w(u)$ corresponding to two surface zero modes $v_{\mathbf{k}_\parallel, x_\perp} = U_\chi(0, w_{\mathbf{k}_\parallel, x_\perp}^T)^T (v_{\mathbf{k}_\parallel, x_\perp} = U_\chi(u_{\mathbf{k}_\parallel, x_\perp}^T, 0))$ with chiral eigenvalue $-1(1)$. Therefore, the generic number of surface zero modes at a fixed \mathbf{k}_\parallel on one surface, if exist, is two and those two modes are chiral eigenstates of the same chiral eigenvalues.

2 Symmetries of Surface Zero Modes

Now we will show the symmetry properties of the surface zero modes. We take $v_{i, \mathbf{k}_\parallel, x_\perp}$ with $i = 1, 2$ as the two orthonormal surface wavefunctions that satisfies Eq. (56) at \mathbf{k}_\parallel with the boundary conditions. Orthonormality requires

$$\int_{-\infty}^0 dx_\perp v_{i, \mathbf{k}_\parallel, x_\perp}^\dagger v_{j, \mathbf{k}_\parallel, x_\perp} = \delta_{ij} . \quad (70)$$

The creation operators of surface modes read

$$b_{i, \mathbf{k}_\parallel}^\dagger = \int_{-\infty}^0 dx_\perp \Psi_{\mathbf{k}_\parallel, x_\perp}^\dagger v_{i, \mathbf{k}_\parallel, x_\perp} , \quad (71)$$

and the orthonormal condition of $v_{i, \mathbf{k}_\parallel, x_\perp}$ leads to the anti-commutation relations

$$\{b_{i, \mathbf{k}_\parallel}^\dagger, b_{j, \mathbf{k}'_\parallel}\} = \delta_{ij} \delta_{\mathbf{k}_\parallel, \mathbf{k}'_\parallel} . \quad (72)$$

The effective Hamiltonian for the surface zero modes can thus be expressed as

$$H_{surf} = E_{surf} \sum_{\mathbf{k}_\parallel \in A} b_{\mathbf{k}_\parallel}^\dagger b_{\mathbf{k}_\parallel} , \quad (73)$$

where A stands for the entire surface mode regions in the surface Brillouin zone, $E_{surf} = 0$ and $b_{\mathbf{k}_\parallel}^\dagger = (b_{1, \mathbf{k}_\parallel}^\dagger, b_{2, \mathbf{k}_\parallel}^\dagger)$. Fermion parity operator will transform the $b_{\mathbf{k}_\parallel}$ operators as $b_{\mathbf{k}_\parallel}^\dagger \rightarrow -b_{\mathbf{k}_\parallel}^\dagger$ and $b_{\mathbf{k}_\parallel} \rightarrow -b_{\mathbf{k}_\parallel}$. The 2D translation read $\hat{T}_{\mathbf{x}_\parallel} b_{\mathbf{k}_\parallel}^\dagger \hat{T}_{\mathbf{x}_\parallel}^{-1} = e^{-i\mathbf{k}_\parallel \cdot \mathbf{x}_\parallel} b_{\mathbf{k}_\parallel}^\dagger$ and $\hat{T}_{\mathbf{x}_\parallel} b_{\mathbf{k}_\parallel} \hat{T}_{\mathbf{x}_\parallel}^{-1} = e^{i\mathbf{k}_\parallel \cdot \mathbf{x}_\parallel} b_{\mathbf{k}_\parallel}$. Due to the TR symmetry, two orthonormal surface wavefunctions $v_{i, -\mathbf{k}_\parallel, x_\perp}$ at $-\mathbf{k}_\parallel$ can be given by the linear combinations of $\mathcal{T}v_{i, \mathbf{k}_\parallel, x_\perp}^*$. Due to $\{\mathcal{T}K, \chi\} = 0$, $v_{i, -\mathbf{k}_\parallel, x_\perp}$ and $v_{i, \mathbf{k}_\parallel, x_\perp}$ have opposite chiral eigenvalues. It means that A_\pm can be related by $\mathbf{k}_\parallel \rightarrow -\mathbf{k}_\parallel$, where A_\pm are the surface mode regions in the \mathbf{k}_\parallel space that are filled with the momenta of surface zero modes with chiral eigenvalue ± 1 , respectively. Based on the same logic,

C_{3v} symmetries gives that $v_{i, C_3 \mathbf{k}_\parallel, x_\perp}$ are linear combinations of $\tilde{C}_3 v_{i, \mathbf{k}_\parallel, x_\perp}$ and $v_{i, \Pi \mathbf{k}_\parallel, x_\perp}$ are linear combinations of $\tilde{\Pi} v_{i, \mathbf{k}_\parallel, x_\perp}$. Furthermore, since χ commutes with any operation in C_{3v} , $v_{i, C_3 \mathbf{k}_\parallel, x_\perp}$'s and $v_{i, \Pi \mathbf{k}_\parallel, x_\perp}$'s have the same chiral eigenvalue as $v_{i, \mathbf{k}_\parallel, x_\perp}$, meaning that both A_+ and A_- are C_{3v} symmetric. The representations of $\hat{\mathcal{T}}$, \hat{C}_3 and $\hat{\Pi}$ rely on the convention that we choose for $v_{i, \mathbf{k}_\parallel, x_\perp}$'s. For convenience, we choose a special convention such that

$$\begin{cases} \mathcal{T} v_{i, \mathbf{k}_\parallel, x_\perp}^* = \sum_j v_{j, -\mathbf{k}_\parallel, x_\perp} (i\sigma_2)_{ji} \\ \tilde{C}_3 v_{i, \mathbf{k}_\parallel, x_\perp} = \sum_j v_{j, C_3 \mathbf{k}_\parallel, x_\perp} (e^{-i\sigma_3 \frac{\pi}{3}})_{ji} \\ \tilde{\Pi} v_{i, \mathbf{k}_\parallel, x_\perp} = \sum_j v_{j, \Pi \mathbf{k}_\parallel, x_\perp} (-e^{-i\sigma_2 \frac{\pi}{2}})_{ji} \end{cases} . \quad (74)$$

As a result, $b_{\mathbf{k}_\parallel}^\dagger$ imitates a $j = 1/2$ fermion:

$$\begin{cases} \hat{\mathcal{T}} b_{\mathbf{k}_\parallel}^\dagger \hat{\mathcal{T}}^{-1} = b_{-\mathbf{k}_\parallel}^\dagger i\sigma_2 \\ \hat{C}_3 b_{\mathbf{k}_\parallel}^\dagger \hat{C}_3^{-1} = b_{C_3 \mathbf{k}_\parallel}^\dagger e^{-i\sigma_3 \frac{\pi}{3}} \\ \hat{\Pi} b_{\mathbf{k}_\parallel}^\dagger \hat{\Pi}^{-1} = b_{\Pi \mathbf{k}_\parallel}^\dagger (-e^{-i\sigma_2 \frac{\pi}{2}}) \end{cases} , \quad (75)$$

where $\sigma_{1,2,3}$ are Pauli matrices for the double degeneracy of the surface modes. And we can treat the double degeneracy of the surface modes as the pseudospin of the surface modes. Since the PH symmetry is related with TR and chiral symmetries by $\chi = i\mathcal{T}C^*$, we have

$$v_{i, -\mathbf{k}_\parallel, x_\perp} = \sum_{j=1}^2 \mathcal{C} v_{j, \mathbf{k}_\parallel, x_\perp}^* (\delta_{\mathbf{k}_\parallel}^\chi \sigma_2)_{ji} , \quad (76)$$

where $\delta_{\mathbf{k}_\parallel}^\chi = \pm 1$ for $\mathbf{k}_\parallel \in A_\pm$, $\chi v_{i, \mathbf{k}_\parallel, x_\perp} = \delta_{\mathbf{k}_\parallel}^\chi v_{i, \mathbf{k}_\parallel, x_\perp}$, $\delta_{-\mathbf{k}_\parallel}^\chi = -\delta_{\mathbf{k}_\parallel}^\chi$ since $v_{i, \mathbf{k}_\parallel, x_\perp}$ and $v_{i, -\mathbf{k}_\parallel, x_\perp}$ have opposite chiral eigenvalues, and $\delta_{R\mathbf{k}_\parallel}^\chi = \delta_{\mathbf{k}_\parallel}^\chi$ with $R \in C_{3v}$ since $v_{i, \mathbf{k}_\parallel, x_\perp}$ and $v_{i, R\mathbf{k}_\parallel, x_\perp}$ have the same chiral eigenvalue. Furthermore, using $\Psi_{-\mathbf{k}_\parallel, x_\perp}^\dagger = \Psi_{\mathbf{k}_\parallel, x_\perp}^T \mathcal{C}$, we can get

$$b_{-\mathbf{k}_\parallel}^\dagger = b_{\mathbf{k}_\parallel}^T (\delta_{\mathbf{k}_\parallel}^\chi \sigma_2) \Leftrightarrow b_{\mathbf{k}_\parallel}^\dagger (-\delta_{\mathbf{k}_\parallel}^\chi \sigma_2) = b_{-\mathbf{k}_\parallel}^T . \quad (77)$$

Thus, the PH symmetry gives rise to the following relation

$$\{b_{i, \mathbf{k}_\parallel}^\dagger, b_{j, \mathbf{k}'_\parallel}^\dagger\} = \{b_{i, \mathbf{k}_\parallel}^\dagger, b_{i', -\mathbf{k}'_\parallel} (\delta_{-\mathbf{k}'_\parallel}^\chi \sigma_2)_{i'j}\} \quad (78)$$

$$= (\delta_{\mathbf{k}_\parallel}^\chi \sigma_2)_{ij} \delta_{\mathbf{k}_\parallel, -\mathbf{k}'_\parallel} , \quad (79)$$

which implies that only half the surface modes are actually physical due to the double counting of the BdG Hamiltonian. In this case, we can treat the surface modes as two Majorana zero modes (MZMs) at each \mathbf{k}_\parallel as described below. In general, the fermionic creation operator $b_{i, \mathbf{k}_\parallel}^\dagger$ can be expressed as the linear combination of two Majorana operators: $b_{i, \mathbf{k}_\parallel}^\dagger = \frac{1}{2}(\gamma_{i, \mathbf{k}_\parallel} + i\tilde{\gamma}_{i, \mathbf{k}_\parallel})$, where

$$\gamma_{i, \mathbf{k}_\parallel} = b_{i, \mathbf{k}_\parallel}^\dagger + b_{i, \mathbf{k}_\parallel} , \quad (80)$$

and $\tilde{\gamma}_{i,\mathbf{k}_\parallel} = \frac{1}{i}(b_{i,\mathbf{k}_\parallel}^\dagger - b_{i,\mathbf{k}_\parallel})$. Due to Eq. (7), $\gamma_{i,\mathbf{k}_\parallel}$ and $\tilde{\gamma}_{i,\mathbf{k}_\parallel}$ depend on each other by the relation $\gamma_{i,-\mathbf{k}_\parallel} = -\delta_{\mathbf{k}_\parallel}^X \sum_j \tilde{\gamma}_{j,\mathbf{k}_\parallel} (i\sigma_2)_{ji}$. Therefore, $\tilde{\gamma}_{i,\mathbf{k}_\parallel}$'s can be chosen to be redundant and we can treat the physical degrees of freedom as two MZMs at each \mathbf{k}_\parallel , of which the Majorana operators are $\gamma_{i,\mathbf{k}_\parallel}$. And the $\gamma_{i,\mathbf{k}_\parallel}$ operators satisfy the following anti-commutation relation:

$$\begin{aligned} \{\gamma_{i,\mathbf{k}_\parallel}, \gamma_{j,\mathbf{k}'_\parallel}\} &= \\ \{b_{i,\mathbf{k}_\parallel}^\dagger, b_{j,\mathbf{k}'_\parallel}^\dagger\} &+ \{b_{i,\mathbf{k}_\parallel}^\dagger, b_{j,\mathbf{k}'_\parallel}\} + \{b_{i,\mathbf{k}_\parallel}, b_{j,\mathbf{k}'_\parallel}^\dagger\} + \{b_{i,\mathbf{k}_\parallel}, b_{j,\mathbf{k}'_\parallel}\} \\ &= 2\delta_{ij}\delta_{\mathbf{k}_\parallel,\mathbf{k}'_\parallel} + (\delta_{\mathbf{k}_\parallel}^X \sigma_2)_{ij}\delta_{\mathbf{k}_\parallel,-\mathbf{k}'_\parallel} + (\delta_{\mathbf{k}_\parallel}^X \sigma_2)_{ij}^* \delta_{\mathbf{k}_\parallel,-\mathbf{k}'_\parallel} \\ &= 2\delta_{ij}\delta_{\mathbf{k}_\parallel,\mathbf{k}'_\parallel}. \end{aligned} \quad (81)$$

Although the actual physical degrees of freedom are MZMs, we still use $b_{\mathbf{k}_\parallel}^\dagger$ and $b_{\mathbf{k}_\parallel}$ in the following for convenience.

Appendix D Projecting Eq. (11) onto the surface to get Eq. (8)

In this part, we will derive Eq. (8) by projecting Eq. (11) onto the surface. First, we show the relation between the surface modes b^\dagger and the Nambu bases Ψ^\dagger . Due to the completeness of eigenstates of Hermitian operator, $\Psi_{\mathbf{k}_\parallel,x_\perp,\alpha,s}^\dagger$ and $\Psi_{\mathbf{k}_\parallel,x_\perp,\alpha,s}$ can be expressed in terms of eigenstates of Eq. (53) for $x_\perp < 0$ and $\mathbf{k}_\parallel \in A$:

$$\begin{cases} \Psi_{\mathbf{k}_\parallel,x_\perp,\alpha,s}^\dagger = \sum_i v_{i,\mathbf{k}_\parallel,x_\perp,\alpha,s}^* b_{i,\mathbf{k}_\parallel}^\dagger + \text{bulk modes} \\ \Psi_{\mathbf{k}_\parallel,x_\perp,\alpha,s} = \sum_i v_{i,\mathbf{k}_\parallel,x_\perp,\alpha,s} b_{i,\mathbf{k}_\parallel} + \text{bulk modes} \end{cases}, \quad (82)$$

where $\alpha = e, h$ is the particle-hole index and $s = \pm\frac{3}{2}, \pm\frac{1}{2}$. Let us define $v_{\mathbf{k}_\parallel,x_\perp}$ as a 8×2 matrix with (α, s) labeling the row and i being the column index, and then the above relations can be expressed in the matrix version:

$$\begin{cases} \Psi_{\mathbf{k}_\parallel,x_\perp}^\dagger = b_{\mathbf{k}_\parallel}^\dagger v_{\mathbf{k}_\parallel,x_\perp}^\dagger + \text{bulk modes} \\ \Psi_{\mathbf{k}_\parallel,x_\perp} = v_{\mathbf{k}_\parallel,x_\perp} b_{\mathbf{k}_\parallel} + \text{bulk modes} \end{cases}. \quad (83)$$

In the matrix version, the symmetries of the surface eigenvectors become

$$\begin{cases} \mathcal{T} v_{\mathbf{k}_\parallel,x_\perp}^* = v_{-\mathbf{k}_\parallel,x_\perp} \mathcal{T}_b \\ \tilde{C}_3 v_{\mathbf{k}_\parallel,x_\perp} = v_{C_3 \mathbf{k}_\parallel,x_\perp} C_{3,b} \\ \tilde{\Pi} v_{\mathbf{k}_\parallel,x_\perp} = v_{\Pi \mathbf{k}_\parallel,x_\perp} \Pi_b \\ v_{-\mathbf{k}_\parallel,x_\perp} = C v_{\mathbf{k}_\parallel,x_\perp}^* \delta_{\mathbf{k}_\parallel}^X \sigma_2 \\ \chi v_{\mathbf{k}_\parallel,x_\perp} = \delta_{\mathbf{k}_\parallel}^X v_{\mathbf{k}_\parallel,x_\perp} \end{cases}. \quad (84)$$

If \mathbf{k}_\parallel is outside the surface mode regions, $\Psi_{\mathbf{k}_\parallel,x_\perp,\alpha,s}^\dagger$ and $\Psi_{\mathbf{k}_\parallel,x_\perp,\alpha,s}$ only contain bulk modes.

In the Nambu bases, Eq. (11) reads

$$\tilde{H}_{mf} = \frac{1}{2} \sum_{\mathbf{k}_\parallel} \int_{-\infty}^0 dx_\perp \Psi_{\mathbf{k}_\parallel,x_\perp}^\dagger \tilde{h}(x_\perp) \Psi_{\mathbf{k}_\parallel,x_\perp} + \text{const.}, \quad (85)$$

where

$$\tilde{h}(x_\perp) = \begin{pmatrix} \tilde{M}(x_\perp) & \tilde{D}(x_\perp) \\ \tilde{D}^\dagger(x_\perp) & -\tilde{M}^T(x_\perp) \end{pmatrix}. \quad (86)$$

Using Eq. (83) and neglecting terms involving bulk modes, we can obtain Eq. (8) with $m(\mathbf{k}_\parallel) = \int_{-\infty}^0 dx_\perp v_{\mathbf{k}_\parallel,x_\perp}^\dagger \tilde{h}(x_\perp) v_{\mathbf{k}_\parallel,x_\perp}$ being Hermitian. Due to the PH symmetry of $\tilde{h}(x_\perp)$, i.e. $-\mathcal{C} \tilde{h}^T(x_\perp) \mathcal{C}^\dagger = \tilde{h}(x_\perp)$, and $v_{\mathbf{k}_\parallel,x_\perp}$ in Eq. (84), the obtained $m(\mathbf{k}_\parallel)$ is PH symmetric. Only the TR odd part of $m(\mathbf{k}_\parallel)$, as well as $\tilde{h}(x_\perp)$, is allowed for the surface orders and thereby we only need to consider $\tilde{h}(x_\perp)$ satisfying $\mathcal{T} \tilde{h}^*(x_\perp) \mathcal{T}^\dagger = -\tilde{h}(x_\perp)$, which is equivalent to $\gamma \tilde{M}^*(x_\perp) \gamma^\dagger = -\tilde{M}(x_\perp)$ and $\gamma \tilde{D}^*(x_\perp) \gamma^T = -\tilde{D}(x_\perp)$. Suppose $\tilde{h}(x_\perp)$ is the linear combination of $\tilde{h}_i(x_\perp)$ and $\tilde{R} \tilde{h}_i(x_\perp) \tilde{R}^\dagger = \sum_j f_{ij} \tilde{h}_j(x_\perp)$ with $f_{ij} \in \mathbb{R}$, where the latter is equivalent to $R \tilde{M}_i(x_\perp) R^\dagger = f_{ij} \tilde{M}_j(x_\perp)$ and $R \tilde{D}_i(x_\perp) R^T = f_{ij} \tilde{D}_j(x_\perp)$, and $R \in C_{3v}$. According to the transformation of $v_{\mathbf{k}_\parallel,x_\perp}$ under C_{3v} (84), we have $R_b \tilde{m}_i(R^{-1} \mathbf{k}_\parallel) R_b^\dagger = \sum_j f_{ij} \tilde{m}_j(\mathbf{k}_\parallel)$, where $\tilde{m}_i(\mathbf{k}_\parallel)$ is the surface projection of $\tilde{h}_i(x_\perp)$. Therefore, if $\tilde{h}_i(x_\perp)$, or equivalently $\tilde{M}_i(x_\perp)$ and $\tilde{D}_i(x_\perp)$, belongs to a certain IR of C_{3v} , the corresponding surface projection belongs to the same IR.

Appendix E Arcs of Majorana Zero Modes

In this section, we will discuss the condition for the arcs of MZMs in the \mathbf{k}_\parallel -space induced by order parameters. The analysis in Sec. IV only included orders that are uniform in each $A_{l_\chi l_c}$, and thereby the surface zero modes either exist or disappear at all \mathbf{k}_\parallel points in one $A_{l_\chi l_c}$ simultaneously. If the momentum dependence of the orders within each $A_{l_\chi l_c}$ is considered, it is possible that MZMs exist at lines in the surface mode regions. To illustrate that, we consider the A_2 order parameter to the linear order of momentum, which has no MZMs according to the analysis in Sec. IV. To take into account the momentum dependence inside $A_{l_\chi l_c}$, we define $\mathbf{K}_\parallel^{l_\chi, l_c}$ to be the geometric center of A_{l_χ, l_c} , and define $h_{A_2}^{l_\chi, l_c}(\mathbf{q}_\parallel) \equiv m_{A_2}(\mathbf{q}_\parallel + \mathbf{K}_\parallel^{l_\chi, l_c})$ with $\mathbf{q}_\parallel \equiv \mathbf{k}_\parallel - \mathbf{K}_\parallel^{l_\chi, l_c}$. Due to the odd mirror parity of A_2 order parameter and the Π symmetry of $A_{+,3}$, $h_{A_2}^{+,3}(\mathbf{q}_\parallel)$ to the first order of \mathbf{q}_\parallel is

$$h_{A_2}^{+,3}(\mathbf{q}_\parallel) = B_0 q_{\parallel,2} \sigma_0 + (-m_4 + B_1 q_{\parallel,1}) \sigma_1 + (-B_2 q_{\parallel,2}) \sigma_2 + (m_3 + B_3 q_{\parallel,1}) \sigma_3, \quad (87)$$

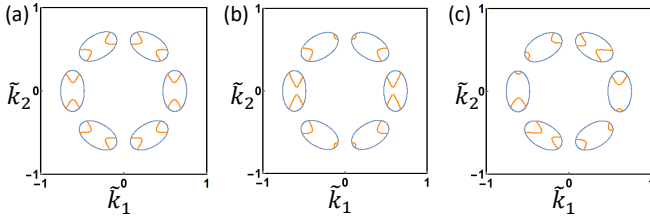


FIG. 5. (a),(b) and (c) show the distribution of surface MZMs in the presence of A_2 surface translationally invariant order parameter without the E order parameters, with the Π anti-symmetric component of E order parameters and with the Π symmetric component of E order parameters, respectively. Blue lines are the boundaries of surface mode regions shown in Fig. 1 and one MZM exists on each point of orange lines. $m_3/|\mu| = 0.05$, $m_4/|\mu| = 0.04$, $B_0\sqrt{2m/\mu} = 0.8$, $B_1\sqrt{2m/\mu} = B_3\sqrt{2m/\mu} = 1$ and $B_2\sqrt{2m/\mu} = -0.5$ are chosen for (a),(b) and (c), while $(m_{7,1}/|\mu|, m_{7,2}/|\mu|) = (0, 0)$ for (a), $(m_{7,1}/|\mu|, m_{7,2}/|\mu|) = (0, 0.05)$ for (b) and $(m_{7,1}/|\mu|, m_{7,2}/|\mu|) = (0.05, 0)$ for (c). The non-zero values of $(m_{7,1}/|\mu|, m_{7,2}/|\mu|)$ indicate the existence of E order. The values of all other parameters are the same as Fig. 1.

where $K_{n,2}^{+,3} = 0$ is used. In the following, we assume $B_{1,2,3,4} \neq 0$. Using C_{3v} and PH symmetries, we have $h_{A_2}^{+,1}(\mathbf{q}_{||}) = C_{3,b}h_{A_2}^{+,3}(C_3^{-1}\mathbf{q}_{||})C_{3,b}^\dagger$, $h_{A_2}^{+,2}(\mathbf{q}_{||}) = C_{3,b}^\dagger h_{A_2}^{+,3}(C_3\mathbf{q}_{||})C_{3,b}$, and $h_{A_2}^{-,l_c}(\mathbf{q}_{||}) = -\sigma_2[h_{A_2}^{+,l_c}(-\mathbf{q}_{||})]^T\sigma_2$. As a result, the number of MZMs at $\mathbf{k}_{||}$ is the same as that at $C_3\mathbf{k}_{||}$, $\Pi\mathbf{k}_{||}$ and $-\mathbf{k}_{||}$, and thereby we only need to study the existence of MZMs in $A_{+,3}$. The eigenvalues of $h_{A_2}^{+,3}(\mathbf{q}_{||})$ are

$$B_0q_{||,2} \pm \sqrt{(m_4 - B_1q_{||,1})^2 + (B_2q_{||,2})^2 + (m_3 + B_3q_{||,1})^2}. \quad (88)$$

In the case where $-m_3/B_3 = m_4/B_1$, two MZMs exist at $\mathbf{q}_{||} = (m_4/B_1, 0)$ if $(m_4/B_1, 0) \in A_{+,3}$, and one MZM exists at every other point (in $A_{+,3}$) on the straight line $(m_4/B_1, q_{||,2})$ if $B_0^2 - B_2^2 = 0$ or on the straight lines $(q_{||,1}, \pm\sqrt{\frac{B_3^2+B_2^2}{B_0^2-B_2^2}}(m_4/B_1 - q_{||,1}))$ if $B_0^2 - B_2^2 > 0$. In the case where $-m_3/B_3 \neq m_4/B_1$, one MZM exists at every point on the part of the hyperbolas $(q_{||,1}, \pm\sqrt{\frac{(m_4-B_1q_{||,1})^2+(m_3+B_3q_{||,1})^2}{B_0^2-B_2^2}})$ that is in $A_{+,3}$ if $B_0^2 - B_2^2 > 0$. If none of the conditions listed above are satisfied, no MZMs exist. As an example, Fig. 5a shows the surface Majorana arcs for $B_0^2 - B_2^2 > 0$ and $-m_3/B_3 \neq m_4/B_1$, where only one MZM exists at each point of the arcs and the distribution of MZMs has C_{3v} and PH symmetries as mentioned before. In the plot, we assume only surface order is formed and the bulk nodal lines as well as the boundaries of surface mode regions do not change. Such distribution of Majorana arcs is possible to be generated by surface FM along the (111) direction since it is an A_2 order parameter.

Next we consider how the E order parameter changes the distribution of Majorana arcs. Suppose the surface Majorana arcs exist for the A_2 order which is given by

surface FM in the (111) direction. In this case, the presence of the small E order parameter can be achieved by tuning the surface magnetic moment slightly away from the (111) direction with a weak external magnetic field, which can change the distribution of the surface Majorana arcs. To illustrate that, we add only the momentum independent E order parameter $\mathbf{m}_7 \cdot \mathbf{N}_7$ to the A_2 order $h_{A_2}^{l_{\chi},l_c}(\mathbf{q}_{||})$ for simplicity. If the magnetic moment is tilted to (112) direction, then the system still has odd Π parity, meaning that $m_{7,1} = 0$. In this case, the C_3 symmetry of the distribution of surface Majorana arc is broken while its Π symmetry is preserved, which is exactly shown in Fig. 5b. If the magnetic moment is tilted to (110) direction, then the extra term should be Π symmetric, meaning that $m_{7,2} = 0$. As a result, the entire C_{3v} symmetry of the surface Majorana arc distribution is broken, which matches Fig. 5c.

Appendix F More Details on Impurity Effect

In this section, we will provide more details on the impurity effect of SMFBs.

1 Order Parameters in $\mathbf{r}_{||}$ space

In this part, we will discuss the transformation of order parameters from the $\mathbf{k}_{||}$ space to the $\mathbf{r}_{||}$ space. Let us consider the general order parameters that are independent of $\mathbf{k}_{||}$ in each A_{l_{χ},l_c} , i.e. Eq. (8) with $m(\mathbf{k}_{||})$ having the form Eq. (15). Using Eq. (21) and Eq. (22), we have

$$H_{mf} = \frac{1}{2} \int d\mathbf{r}_{||} d\mathbf{r}_{||}' M d\mathbf{r}_{||}, \quad (89)$$

with $M_{l_{\chi},l_c,l_c',l_c'',ii'} = \sum_{l=0}^3 f_l^{l_{\chi},l_c}(\sigma_l)_{ii'}\delta_{l_{\chi},l_c'}\delta_{l_c,l_c''} \cdot f_l^{l_{\chi},l_c},s$ for different l_{χ},l_c are given by 1 or $\delta_{\mathbf{k}_{||}}^{\alpha}$ with $\alpha = \chi, (E_1, \pm), (E_2, \pm)$. Specifically, we have

$$\begin{aligned} 1 &= \sum_{l_{\chi},l_c} (\rho_0)_{l_{\chi}l_{\chi}} (\Lambda_1)_{l_c l_c} \delta_{\mathbf{k}_{||}}^{l_{\chi},l_c} \\ \delta_{\mathbf{k}_{||}}^{\chi} &= \sum_{l_{\chi},l_c} (\rho_3)_{l_{\chi}l_{\chi}} (\Lambda_1)_{l_c l_c} \delta_{\mathbf{k}_{||}}^{l_{\chi},l_c} \\ \delta_{\mathbf{k}_{||}}^{E_1,+} &= \sum_{l_{\chi},l_c} (\rho_0)_{l_{\chi}l_{\chi}} (\Lambda_{4,1})_{l_c l_c} \delta_{\mathbf{k}_{||}}^{l_{\chi},l_c} \\ \delta_{\mathbf{k}_{||}}^{E_1,-} &= \sum_{l_{\chi},l_c} (\rho_3)_{l_{\chi}l_{\chi}} (\Lambda_{4,1})_{l_c l_c} \delta_{\mathbf{k}_{||}}^{l_{\chi},l_c} \\ \delta_{\mathbf{k}_{||}}^{E_2,+} &= \sum_{l_{\chi},l_c} (\rho_0)_{l_{\chi}l_{\chi}} (\Lambda_{4,2})_{l_c l_c} \delta_{\mathbf{k}_{||}}^{l_{\chi},l_c} \\ \delta_{\mathbf{k}_{||}}^{E_2,-} &= \sum_{l_{\chi},l_c} (\rho_3)_{l_{\chi}l_{\chi}} (\Lambda_{4,2})_{l_c l_c} \delta_{\mathbf{k}_{||}}^{l_{\chi},l_c}, \end{aligned} \quad (90)$$

where that all matrices involved are diagonal due to translation symmetry. Using the above correspondence,

Tab. IV and Eq. (16)-18, we can get

$$H_{mf}^\alpha = \frac{1}{2} \int d^2 \mathbf{r}_\parallel d_{\mathbf{r}_\parallel}^\dagger M_\alpha d_{\mathbf{r}_\parallel} + \text{const.}, \quad (91)$$

where $\alpha = A_1, A_2, E$,

$$M_{A_1} = m_1 \rho_3 \otimes \Lambda_1 \otimes \sigma_0 + m_2 (-\rho_0 \otimes \Lambda_{4,1} \otimes \sigma_2 + \rho_0 \otimes \Lambda_{4,2} \otimes \sigma_1), \quad (92)$$

$$M_{A_2} = m_3 \rho_0 \otimes \Lambda_1 \otimes \sigma_3 + m_4 (\rho_0 \otimes \Lambda_{4,2} \otimes \sigma_2 + \rho_0 \otimes \Lambda_{4,1} \otimes \sigma_1), \quad (93)$$

and

$$\begin{aligned} M_E = & m_{5,1} \rho_3 \otimes \Lambda_{4,1} \otimes \sigma_0 + m_{5,2} \rho_3 \otimes \Lambda_{4,2} \otimes \sigma_0 \\ & + m_{6,1} (-\rho_0 \otimes \Lambda_{4,2} \otimes \sigma_3) + m_{6,2} (\rho_0 \otimes \Lambda_{4,1} \otimes \sigma_3) \\ & + m_{7,1} (-\rho_0 \otimes \Lambda_1 \otimes \sigma_2) + m_{7,2} (\rho_0 \otimes \Lambda_1 \otimes \sigma_1) \\ & + m_{8,1} (\rho_0 \otimes \Lambda_{4,1} \otimes \sigma_2 + \rho_0 \otimes \Lambda_{4,2} \otimes \sigma_1) \\ & + m_{8,2} (\rho_0 \otimes \Lambda_{4,1} \otimes \sigma_1 - \rho_0 \otimes \Lambda_{4,2} \otimes \sigma_2). \end{aligned} \quad (94)$$

According to Tab. I, Eq. (92), Eq. (93) and Eq. (94) are the most general PH symmetric uniform order parameters for the A_1 , A_2 and E IRs.

2 Verification of LDOS Peaks for Translational Invariant Order Parameters with d Bases

The purpose for this section is to re-derive the distribution of LDOS peaks from the symmetry aspect of the order parameters in Eq. (92)-94 with the d bases and establish the formalism that can be generalized to the case with charge/magnetic impurities. Since the position \mathbf{r}_\parallel is now approximately a good quantum number, the number of LDOS peaks is directly determined by the number of different eigenvalues of M_α . It means that the numbers of LDOS peaks far away from impurities should be typically 1,4,2 and 12 for no order parameters, the A_1 order parameter, the A_2 order parameter and the E order parameter, respectively, as indicated in Sec. IV. 12 LDOS peaks for the E order parameter are justified by the fact that M_α 's are all 12×12 matrices with 12 eigenvalues and the E order parameter typically has no symmetries to ensure any degeneracy. To discuss A_1 and A_2 order parameters, we again transform all the symmetry operators to the eigenbases of $C_{3,d}$ as discussed in the main text. By choosing the same convention (28,29) in the main text, the representations of the symmetry operations other than \hat{C}_3 and $\hat{\Pi}$ are

$$\tilde{U}_T = \begin{pmatrix} & & \mathbb{1}_4 \\ & & \\ & & \mathbb{1}_4 \\ \mathbb{1}_4 & & \end{pmatrix}, \quad (95)$$

$$\tilde{C}_d = \begin{pmatrix} & U_c \\ & U_c \\ U_c & \end{pmatrix} \quad (96)$$

with

$$U_c = \begin{pmatrix} 0 & 0 & 0 & i \\ 0 & 0 & -i & 0 \\ 0 & -i & 0 & 0 \\ i & 0 & 0 & 0 \end{pmatrix}, \quad (97)$$

and

$$\tilde{\chi}_d = \begin{pmatrix} U_\chi & & \\ & U_\chi & \\ & & U_\chi \end{pmatrix} \quad (98)$$

with

$$U_\chi = \begin{pmatrix} -1 & 0 & 0 & 0 \\ 0 & -1 & 0 & 0 \\ 0 & 0 & 1 & 0 \\ 0 & 0 & 0 & 1 \end{pmatrix}, \quad (99)$$

where \tilde{R} means the matrix form of R in the $C_{3,d}$ eigenbases and U_T is defined such that M is diagonal for l_c index if and only if $[M, U_T] = 0$. The A_1 order parameter satisfies $[M_{A_1}, C_{3,d}] = [M_{A_1}, U_T] = 0$. Due to the commutation relation with $C_{3,d}$, \tilde{M}_{A_1} should be block-diagonal and written as $\tilde{M}_{A_1} = \text{diag}(h_1, h_2, h_3)$, where $h_{1,2,3}$ are Hermitian 4×4 matrices. Furthermore, due to the commutation relation with U_T , we requires $h_1 = h_2 = h_3$, which leads to the three-fold degeneracy of each eigenvalues. As a result, M_{A_1} has typically 4 LDOS peaks. The A_2 order parameter satisfies not only $[M_{A_2}, C_{3,d}] = [M_{A_2}, U_T] = 0$ but also $[M_{A_2}, \Pi_d C_d K] = 0$, in which we have $(\Pi_d C_d K)^2 = -1$. The former leads to $\tilde{M}_{A_2} = \text{diag}(h_1, h_1, h_1)$ as mentioned above, while $\Pi_d C_d M^* C_d^\dagger \Pi_d^\dagger = M$ results in $U_\Pi U_c h_1^* U_c^\dagger U_\Pi^\dagger = h_1$. Thereby, each eigenvalues of h_1 have double degeneracy due to $U_\Pi U_c (U_\Pi U_c)^* = -1$. As a result, all eigenvalues of M_{A_2} have six-fold degeneracy and the A_2 order parameter typically has 2 peaks. In addition, M_α 's are PH symmetric, which guarantees that LDOS peaks are symmetric with respect to zero energy.

3 Derivation of Eq. (26) and the Symmetry Properties

In this part, we will derive Eq. (26) and discuss the corresponding symmetry properties. The surface impurity Hamiltonian that we consider has the general form

$$H_V = \int d^3 \mathbf{r} c_{\mathbf{r}}^\dagger V(\mathbf{r}) c_{\mathbf{r}}, \quad (100)$$

where the position of the impurity is at $\mathbf{r} = 0$ (certainly on the $x_\perp = 0$ surface) and $V(\mathbf{r})^\dagger = V(\mathbf{r})$ decays fast

away from $\mathbf{r} = 0$. First we express Eq.(100) in the Nambu bases as

$$H_V = \frac{1}{2} \int d^2 r_{||} \int dx_{\perp} \frac{1}{S_{||}} \sum_{\mathbf{k}_{||}, \mathbf{k}'_{||}} e^{-i\mathbf{k}_{||} \cdot \mathbf{r}_{||} + i\mathbf{k}'_{||} \cdot \mathbf{r}_{||}} \Psi_{\mathbf{k}_{||}, x_{\perp}}^{\dagger} \tilde{V}(\mathbf{r}) \Psi_{\mathbf{k}'_{||}, x_{\perp}} + \text{const.}, \quad (101)$$

where

$$\tilde{V}(\mathbf{r}) = \begin{pmatrix} V(\mathbf{r}) & \\ & -V^*(\mathbf{r}) \end{pmatrix}, \quad (102)$$

and $\Psi_{\mathbf{r}}^{\dagger} = \frac{1}{\sqrt{S_{||}}} \sum_{\mathbf{k}_{||}} e^{-i\mathbf{k}_{||} \cdot \mathbf{r}_{||}} \Psi_{\mathbf{k}_{||}, x_{\perp}}^{\dagger}$ is used. Using Eq.(83), we only keep terms that involve surface modes and assume $v_{\mathbf{k}_{||}, x_{\perp}} \approx v_{\mathbf{K}_{||}^{l_{\chi}, l_c}, x_{\perp}}$ for all $\mathbf{k}_{||} \in A_{l_{\chi}, l_c}$ and all l_{χ}, l_c . This leads to Eq.(26) with

$$[M_V(\mathbf{r}_{||})]_{l_{\chi} l'_{\chi}, l_c l'_c, ii'} = \int_{-\infty}^0 dx_{\perp} v_{i, \mathbf{K}_{||}^{l_{\chi}, l_c}, x_{\perp}}^{\dagger} \tilde{V}(\mathbf{r}) v_{i', \mathbf{K}_{||}^{l'_{\chi}, l'_c}, x_{\perp}}. \quad (103)$$

Since $V^{\dagger}(\mathbf{r}) = V(\mathbf{r})$, we have $M_V^{\dagger}(\mathbf{r}_{||}) = M_V(\mathbf{r}_{||})$. Due to

$$\sum_{l'_{\chi}, l'_c, i'} [\mathcal{C}_d]_{l_{\chi} l'_{\chi}, l_c l'_c, ii'} v_{i', \mathbf{K}_{||}^{l'_{\chi}, l'_c}, x_{\perp}} = \mathcal{C}_v^*_{i, \mathbf{K}_{||}^{l_{\chi}, l_c}, x_{\perp}}, \quad (104)$$

$M_V(\mathbf{r}_{||})$ is PH symmetric, written as

$$-\mathcal{C}_d M_V^T(\mathbf{r}_{||}) \mathcal{C}_d^{\dagger} = M_V(\mathbf{r}_{||}). \quad (105)$$

Due to

$$\sum_{l'_{\chi}, l'_c, i'} [\mathcal{T}_d]_{l_{\chi} l'_{\chi}, l_c l'_c, ii'} v_{i', \mathbf{K}_{||}^{l'_{\chi}, l'_c}, x_{\perp}} = \mathcal{T}^T v^*_{i, \mathbf{K}_{||}^{l_{\chi}, l_c}, x_{\perp}}, \quad (106)$$

$M_V(\mathbf{r}_{||})$ has the same TR properties as $\tilde{V}(\mathbf{r})$:

$$[\mathcal{T}_d M_V^*(\mathbf{r}_{||}) \mathcal{T}_d^{\dagger}]_{l_{\chi} l'_{\chi}, l_c l'_c, ii'} = \int_{-\infty}^0 dx_{\perp} v_{i, \mathbf{K}_{||}^{l_{\chi}, l_c}, x_{\perp}}^{\dagger} \mathcal{T} \tilde{V}^*(\mathbf{r}) \mathcal{T}^{\dagger} v_{i', \mathbf{K}_{||}^{l'_{\chi}, l'_c}, x_{\perp}}. \quad (107)$$

Similarly, due to

$$\sum_{l'_{\chi}, l'_c, i'} [R_d]_{l_{\chi} l'_{\chi}, l_c l'_c, ii'} v_{i', \mathbf{K}_{||}^{l'_{\chi}, l'_c}, x_{\perp}}^{\dagger} = v_{i, \mathbf{K}_{||}^{l_{\chi}, l_c}, x_{\perp}}^{\dagger} \tilde{R}, \quad (108)$$

$M_V(\mathbf{r}_{||})$ has the same C_{3v} properties as $\tilde{V}(\mathbf{r})$:

$$[\mathcal{R}_d M_V(\mathbf{r}_{||}) \mathcal{R}_d^{\dagger}]_{l_{\chi} l'_{\chi}, l_c l'_c, ii'} = \int_{-\infty}^0 dx_{\perp} v_{i, \mathbf{K}_{||}^{l_{\chi}, l_c}, x_{\perp}}^{\dagger} \tilde{R} \tilde{V}(\mathbf{r}) \tilde{R}^{\dagger} v_{i', \mathbf{K}_{||}^{l'_{\chi}, l'_c}, x_{\perp}}, \quad (109)$$

where $R \in C_{3v}$. Furthermore, since $\tilde{V}(\mathbf{r})$ behaves the same as $V(\mathbf{r})$, the TR and C_{3v} properties of $M_V(\mathbf{r}_{||})$ are the same as those of $V(\mathbf{r})$.

For a charge impurity, $V(\mathbf{r}) = V_c(\mathbf{r}) \mathbb{1}_{4 \times 4}$ with $V_c(\mathbf{r})$ a real scalar function. In this case, $V_c(\mathbf{r}) \mathbb{1}_{4 \times 4}$ has TR symmetry $\gamma(V_c(\mathbf{r}) \mathbb{1}_{4 \times 4})^* \gamma^{\dagger} = V_c(\mathbf{r}) \mathbb{1}_{4 \times 4}$ and satisfies $R(V_c(\mathbf{r}) \mathbb{1}_{4 \times 4}) R^{\dagger} = V_c(\mathbf{r}) \mathbb{1}_{4 \times 4}$ with $R \in C_{3v}$. As a result, Hermitian and PH symmetric $M_V(\mathbf{r})$ has TR symmetry $\mathcal{T}_d M_V^*(\mathbf{r}_{||}) \mathcal{T}_d^{\dagger} = M_V(\mathbf{r}_{||})$ and satisfies $R_d M_V(\mathbf{r}_{||}) R_d^{\dagger} = M_V(\mathbf{r}_{||})$ with $R \in C_{3v}$. Combining TR and PH symmetries, we have chiral symmetry for $M_V(\mathbf{r}_{||})$, i.e. $\chi_d M_V(\mathbf{r}_{||}) \chi_d^{\dagger} = -M_V(\mathbf{r}_{||})$. By defining $M_c = M_V(\mathbf{r}_{||} = 0)$, the symmetry properties of M_c can be directly obtained.

For a magnetic impurity, we choose the magnetic moment of the impurity to be perpendicular to the surface and couple to the electron spin locally, i.e. choosing $V(\mathbf{r}) = V_m(\mathbf{r}) \mathbf{e}_{\perp} \cdot \mathbf{J}$ with $V_m(\mathbf{r})$ a real scalar function and $\mathbf{e}_{\perp} = (1, 1, 1)/\sqrt{3}$. In this case, $V_m(\mathbf{r}) \mathbf{e}_{\perp} \cdot \mathbf{J}$ is TR odd $\gamma(V_m(\mathbf{r}) \mathbf{e}_{\perp} \cdot \mathbf{J})^* \gamma^{\dagger} = -V_m(\mathbf{r}) \mathbf{e}_{\perp} \cdot \mathbf{J}$, and satisfies $C_3(V_m(\mathbf{r}) \mathbf{e}_{\perp} \cdot \mathbf{J}) C_3^{\dagger} = V_m(\mathbf{r}) \mathbf{e}_{\perp} \cdot \mathbf{J}$ and $\Pi(V_m(\mathbf{r}) \mathbf{e}_{\perp} \cdot \mathbf{J}) \Pi^{\dagger} = -V_m(\mathbf{r}) \mathbf{e}_{\perp} \cdot \mathbf{J}$. As a result, the Hermitian and PH symmetric $M_V(\mathbf{r}_{||})$ has TR antisymmetry $\mathcal{T}_d M_V^*(\mathbf{r}_{||}) \mathcal{T}_d^{\dagger} = -M_V(\mathbf{r}_{||})$, and satisfies $C_{3,d} M_V(\mathbf{r}_{||}) C_{3,d}^{\dagger} = M_V(\mathbf{r}_{||})$ and $\Pi_d M_V(\mathbf{r}_{||}) \Pi_d^{\dagger} = -M_V(\mathbf{r}_{||})$. By defining $M_m = M_V(\mathbf{r}_{||} = 0)$, the symmetry properties of M_m can be obtained.

In Fig.3, $V_c(\mathbf{r})/|\mu| = 2/(|\mathbf{r}| \sqrt{2m\mu} + 0.02)^2$ if the charge impurity is considered, and $V_m(\mathbf{r})/|\mu| = 5e^{x_{\perp} \sqrt{2m\mu}/2} \theta(|\mathbf{r}_{||,0}| - |\mathbf{r}_{||}|)$ with $|\mathbf{r}_{||}| < |\mathbf{r}_{||,0}|$ if the magnetic impurity is considered.

* cxl56@psu.edu

¹ H. Kim, K. Wang, Y. Nakajima, R. Hu, S. Ziemak, P. Syers, L. Wang, H. Hodovanets, J. D. Denlinger, P. M. Brydon, *et al.*, arXiv preprint arXiv:1603.03375 (2016).
² T. Graf, S. S. Parkin, and C. Felser, IEEE Transactions on Magnetics **47**, 367 (2011).
³ H. Lin, L. A. Wray, Y. Xia, S. Xu, S. Jia, R. J. Cava, A. Bansil, and M. Z. Hasan, Nature materials **9**, 546 (2010).

⁴ S. Chadov, X. Qi, J. Kübler, G. H. Fecher, C. Felser, and S. C. Zhang, Nature materials **9**, 541 (2010).

⁵ D. Xiao, Y. Yao, W. Feng, J. Wen, W. Zhu, X.-Q. Chen, G. M. Stocks, and Z. Zhang, Phys. Rev. Lett. **105**, 096404 (2010).

⁶ W. Al-Sawai, H. Lin, R. S. Markiewicz, L. A. Wray, Y. Xia, S.-Y. Xu, M. Z. Hasan, and A. Bansil, Phys. Rev. B **82**, 125208 (2010).

⁷ B. Yan and A. de Visser, MRS Bulletin **39**, 859 (2014).

- ⁸ Z. K. Liu, L. X. Yang, S.-C. Wu, C. Shekhar, J. Jiang, H. F. Yang, Y. Zhang, S.-K. Mo, Z. Hussain, B. Yan, C. Felser, and Y. L. Chen, *Nature Communications* **7**, 12924 (2016), article.
- ⁹ J. Logan, S. Patel, S. Harrington, C. Polley, B. Schultz, T. Balasubramanian, A. Janotti, A. Mikkelsen, and C. Palmstrøm, *Nature communications* **7** (2016).
- ¹⁰ J. Cano, B. Bradlyn, Z. Wang, M. Hirschberger, N. Ong, and B. Bernevig, arXiv preprint arXiv:1604.08601 (2016).
- ¹¹ J. Ruan, S.-K. Jian, H. Yao, H. Zhang, S.-C. Zhang, and D. Xing, *Nature communications* **7** (2016).
- ¹² M. Hirschberger, S. Kushwaha, Z. Wang, Q. Gibson, S. Liang, C. A. Belvin, B. A. Bernevig, R. J. Cava, and N. P. Ong, *Nat Mater* **15**, 1161 (2016), letter.
- ¹³ C. Shekhar, A. K. Nayak, S. Singh, N. Kumar, S.-C. Wu, Y. Zhang, A. C. Komarek, E. Kampert, Y. Skourski, J. Wosnitza, *et al.*, arXiv preprint arXiv:1604.01641 (2016).
- ¹⁴ T. Suzuki, R. Chisnell, A. Devarakonda, Y.-T. Liu, W. Feng, D. Xiao, J. Lynn, and J. Checkelsky, *Nature Physics* (2016).
- ¹⁵ H. Yang, J. Yu, S. S. P. Parkin, C. Felser, C.-X. Liu, and B. Yan, *Phys. Rev. Lett.* **119**, 136401 (2017).
- ¹⁶ J. Liu, H. Liu, G. Cao, and Z. Zhou, arXiv preprint arXiv:1808.04748 (2018).
- ¹⁷ Y. Pan, A. M. Nikitin, T. V. Bay, Y. K. Huang, C. Paulsen, B. H. Yan, and A. de Visser, *EPL (Europhysics Letters)* **104**, 27001 (2013).
- ¹⁸ K. Gofryk, D. Kaczorowski, T. Plackowski, A. Leithe-Jasper, and Y. Grin, *Phys. Rev. B* **84**, 035208 (2011).
- ¹⁹ R. A. Müller, N. R. Lee-Hone, L. Lapointe, D. H. Ryan, T. Pereg-Barnea, A. D. Bianchi, Y. Mozharivskyj, and R. Flacau, *Phys. Rev. B* **90**, 041109 (2014).
- ²⁰ A. M. Nikitin, Y. Pan, X. Mao, R. Jehee, G. K. Araizi, Y. K. Huang, C. Paulsen, S. C. Wu, B. H. Yan, and A. de Visser, *Journal of Physics: Condensed Matter* **27**, 275701 (2015).
- ²¹ Y. Nakajima, R. Hu, K. Kirshenbaum, A. Hughes, P. Syers, X. Wang, K. Wang, R. Wang, S. R. Saha, D. Pratt, *et al.*, *Science advances* **1**, e1500242 (2015).
- ²² O. Pavlosiuk, D. Kaczorowski, X. Fabreges, A. Gukasov, and P. Wiśniewski, *Scientific reports* **6** (2016).
- ²³ O. Pavlosiuk, D. Kaczorowski, and P. Wiśniewski, *Acta Physica Polonica A* **130**, 573 (2016).
- ²⁴ J. Yu, B. Yan, and C.-X. Liu, *Phys. Rev. B* **95**, 235158 (2017).
- ²⁵ O. Pavlosiuk, X. Fabreges, A. Gukasov, M. Meven, D. Kaczorowski, and P. Wiśniewski, *Physica B: Condensed Matter* **536**, 56 (2018).
- ²⁶ G. Goll, M. Marz, A. Hamann, T. Tomanic, K. Grube, T. Yoshino, and T. Takabatake, *Physica B: Condensed Matter* **403**, 1065 (2008).
- ²⁷ N. P. Butch, P. Syers, K. Kirshenbaum, A. P. Hope, and J. Paglione, *Phys. Rev. B* **84**, 220504 (2011).
- ²⁸ T. V. Bay, T. Naka, Y. K. Huang, and A. de Visser, *Phys. Rev. B* **86**, 064515 (2012).
- ²⁹ F. F. Tafti, T. Fujii, A. Jumeau-Fecteau, S. René de Cotret, N. Doiron-Leyraud, A. Asamitsu, and L. Taillefer, *Phys. Rev. B* **87**, 184504 (2013).
- ³⁰ G. Xu, W. Wang, X. Zhang, Y. Du, E. Liu, S. Wang, G. Wu, Z. Liu, and X. X. Zhang, *Scientific reports* **4**, 5709 (2014).
- ³¹ O. Pavlosiuk, D. Kaczorowski, and P. Wiśniewski, *Scientific reports* **5**, 9158 (2015).
- ³² M. Meinert, *Phys. Rev. Lett.* **116**, 137001 (2016).
- ³³ H. Xiao, T. Hu, W. Liu, Y. L. Zhu, P. G. Li, G. Mu, J. Su, K. Li, and Z. Q. Mao, *Phys. Rev. B* **97**, 224511 (2018).
- ³⁴ P. M. R. Brydon, L. Wang, M. Weinert, and D. F. Agterberg, *Phys. Rev. Lett.* **116**, 177001 (2016).
- ³⁵ T. Kawakami, T. Okamura, S. Kobayashi, and M. Sato, arXiv preprint arXiv:1802.09962 (2018).
- ³⁶ C. Wu, *Modern Physics Letters B* **20**, 1707 (2006).
- ³⁷ I. Kuzmenko, T. Kuzmenko, Y. Avishai, and M. Sato, arXiv preprint arXiv:1801.05646 (2018).
- ³⁸ W. Yang, T. Xiang, and C. Wu, *Phys. Rev. B* **96**, 144514 (2017).
- ³⁹ C. Timm, A. P. Schnyder, D. F. Agterberg, and P. M. R. Brydon, *Phys. Rev. B* **96**, 094526 (2017).
- ⁴⁰ J. Yu and C.-X. Liu, arXiv preprint arXiv:1801.00083 (2017).
- ⁴¹ Q.-Z. Wang, J. Yu, and C.-X. Liu, arXiv preprint arXiv:1801.10286 (2018).
- ⁴² J. Yu and C.-X. Liu, arXiv preprint arXiv:1809.04736 (2018).
- ⁴³ B. Roy, S. A. A. Ghorashi, M. S. Foster, and A. H. Nev- idomskyy, arXiv preprint arXiv:1708.07825 (2017).
- ⁴⁴ I. Boettcher and I. F. Herbut, *Phys. Rev. Lett.* **120**, 057002 (2018).
- ⁴⁵ W. Yang, Y. Li, and C. Wu, *Phys. Rev. Lett.* **117**, 075301 (2016).
- ⁴⁶ J. W. F. Venderbos, L. Savary, J. Ruhman, P. A. Lee, and L. Fu, *Phys. Rev. X* **8**, 011029 (2018).
- ⁴⁷ L. Savary, J. Ruhman, J. W. F. Venderbos, L. Fu, and P. A. Lee, *Phys. Rev. B* **96**, 214514 (2017).
- ⁴⁸ S. A. A. Ghorashi, S. Davis, and M. S. Foster, *Phys. Rev. B* **95**, 144503 (2017).
- ⁴⁹ P. Brydon, D. Agterberg, H. Menke, and C. Timm, arXiv preprint arXiv:1806.03773 (2018).
- ⁵⁰ K. Yada, M. Sato, Y. Tanaka, and T. Yokoyama, *Phys. Rev. B* **83**, 064505 (2011).
- ⁵¹ Y. Li, D. Wang, and C. Wu, *New Journal of Physics* **15**, 085002 (2013).
- ⁵² A. C. Potter and P. A. Lee, *Phys. Rev. Lett.* **112**, 117002 (2014).
- ⁵³ C. Timm, S. Rex, and P. M. R. Brydon, *Phys. Rev. B* **91**, 180503 (2015).
- ⁵⁴ J. S. Hofmann, F. F. Assaad, and A. P. Schnyder, *Phys. Rev. B* **93**, 201116 (2016).
- ⁵⁵ S. Ikegaya, Y. Asano, and Y. Tanaka, *Phys. Rev. B* **91**, 174511 (2015).
- ⁵⁶ S. Ikegaya and Y. Asano, *Phys. Rev. B* **95**, 214503 (2017).
- ⁵⁷ S. Ikegaya, S. Kobayashi, and Y. Asano, *Phys. Rev. B* **97**, 174501 (2018).
- ⁵⁸ J. M. Luttinger, *Phys. Rev.* **102**, 1030 (1956).
- ⁵⁹ R. Winkler, S. Papadakis, E. De Poortere, and M. Shayegan, *Spin-Orbit Coupling in Two-Dimensional Electron and Hole Systems*, Vol. 41 (Springer, 2003) pp. 211–223.
- ⁶⁰ E. I. Blount, *Phys. Rev. B* **32**, 2935 (1985).
- ⁶¹ K. Ueda and T. M. Rice, *Phys. Rev. B* **31**, 7114 (1985).
- ⁶² G. Volovik and L. Gorkov, *Zhurnal Eksperimentalnoi i Teoreticheskoi Fiziki* **88**, 1412 (1985).
- ⁶³ M. Sigrist and K. Ueda, *Rev. Mod. Phys.* **63**, 239 (1991).
- ⁶⁴ J. F. Annett, *Advances in Physics* **39**, 83 (1990).
- ⁶⁵ J. Annett, N. Goldenfeld, and S. R. Renn, *Phys. Rev. B* **43**, 2778 (1991).
- ⁶⁶ J. F. Annett, N. Goldenfeld, and A. J. Leggett, *Journal of Low Temperature Physics* **105**, 473 (1996).

- ⁶⁷ M. Tinkham, *Introduction to superconductivity* (McGraw-Hill, New York, 1996).
- ⁶⁸ Z. Bi, N. F. Q. Yuan, and L. Fu, [Phys. Rev. B **100**, 035448 \(2019\)](#).
- ⁶⁹ M. Sato, Y. Tanaka, K. Yada, and T. Yokoyama, [Phys. Rev. B **83**, 224511 \(2011\)](#).
- ⁷⁰ S. Murakami, N. Nagosa, and S.-C. Zhang, [Phys. Rev. B **69**, 235206 \(2004\)](#).
- ⁷¹ M. I. Aroyo, A. Kirov, C. Capillas, J. Perez-Mato, and H. Wondratschek, *Acta Crystallographica Section A* **62**, 115 (2006).
- ⁷² M. Gell-Mann, [Phys. Rev. **125**, 1067 \(1962\)](#).